

Published in final edited form as:

Mol Cell Neurosci. 2008 November ; 39(3): 439–451. doi:10.1016/j.mcn.2008.07.027.

Mitochondrial localization and function of a subset of 22q11

Deletion Syndrome candidate genes

T. M. Maynard¹, D. W. Meechan^{1,3}, M. L. Dudevior¹, D. Gopalakrishna¹, A. Z. Peters¹, C. C. Heindel¹, T. J. Sugimoto¹, Y. Wu¹, J. A. Lieberman^{2,†}, and A.-S. LaMantia^{1,2,3}

¹Department of Cell & Molecular Physiology, The University of North Carolina School of Medicine, Chapel Hill NC 27599

²Department of Psychiatry, The University of North Carolina School of Medicine, Chapel Hill NC 27599

³UNC Neuroscience Center, The University of North Carolina School of Medicine, Chapel Hill NC 27599

Abstract

Six genes in the 1.5 MB region of chromosome 22 deleted in DiGeorge/22q11 Deletion Syndrome—*Mprl40*, *Prodh*, *Slc25a1*, *Txnrd2*, *T10*, and *Zdhhc8*—encode mitochondrial proteins. All six genes are expressed in the brain, and maximal expression coincides with peak forebrain synaptogenesis shortly after birth. Furthermore, their protein products are associated with brain mitochondria, including those in synaptic terminals. Among the six, only *Zdhhc8* influences mitochondria-regulated apoptosis when overexpressed, and appears to interact biochemically with established mitochondrial proteins. *Zdhhc8* has an apparent interaction with *Uqcrc1*, a component of mitochondrial complex III. The two proteins are coincidentally expressed in presynaptic processes; however, *Zdhhc8* is more frequently seen in glutamatergic terminals. 22q11 deletion may alter metabolic properties of cortical mitochondria during early post-natal life, since expression complex III components, including *Uqcrc1*, is significantly increased at birth in a mouse model of 22q11 deletion, and declines to normal values in adulthood. Our results suggest that altered dosage of one, or several 22q11 mitochondrial genes, particularly during early postnatal cortical development, may disrupt neuronal metabolism or synaptic signaling.

Introduction

22q11 deletion syndrome (22q11DS) is associated with numerous cognitive and psychiatric disorders (Bassett et al., 1999; Ousley et al., 2007; Ryan et al., 1997), from mild learning disorders to schizophrenia, autism, attention-deficit disorder, and mood disorders. Very little is known about how individual (or sets of) 22q11 genes contribute to the high incidence of these cognitive and psychiatric disorders. In contrast, the relationship between a single 22q11 gene, the transcription factor *Tbx1*, and 22q11DS cardiovascular phenotypes has been clarified

© 2008 Elsevier Inc. All rights reserved.

Corresponding Author: Thomas Maynard, Department of Cell and Molecular Physiology, University of North Carolina, Chapel Hill, 115 Mason Farm Rd. CB#7545, 7105 Neurosciences Research Building, Chapel Hill, NC 27599-7545, Phone: 919 843 8110, Fax: 919 966 6927, Email: tom_maynard@med.unc.edu.

[†]present address: Department of Psychiatry, Columbia University College of Physicians and Surgeons, New York, New York, 10020

Publisher's Disclaimer: This is a PDF file of an unedited manuscript that has been accepted for publication. As a service to our customers we are providing this early version of the manuscript. The manuscript will undergo copyediting, typesetting, and review of the resulting proof before it is published in its final citable form. Please note that during the production process errors may be discovered which could affect the content, and all legal disclaimers that apply to the journal pertain.

by a combination of cellular and tissue expression analysis as well as functional assessment (Jerome et al., 2001; Lindsay et al., 2001; Merscher et al., 2001). Accordingly, we asked whether additional 22q11 genes, selectively influence critical cellular mechanisms in the developing or adult brain that, if disrupted, might contribute to cognitive impairment or psychiatric disease.

The best indication that a subset of individual 22q11 genes could contribute to cognitive disorders comes from linkage studies in schizophrenic patients. Three 22q11 regions repeatedly show associations: *Prodh* and *Dgcr2/Es2* (Li et al., 1996; Liu et al., 2002b; Shifman et al., 2006), the upstream promoter for *Comt* and *Txnrd2* (Palmatier et al., 2004), and a 0.5 Mb multi-gene region in the distal 22q11 minimal region (*Rtn4r-T10*; Liu et al., 2002a). In the latter region, a particular focus has been placed on *Zdhhc8* (Chen et al., 2004; Mukai et al., 2004); however, the region includes five additional genes: *T10*, *Dgcr8*, *Htf9c*, *Ranbp1*, and *Rtn4r*. Two of these risk genes—*Prodh* and *Txnrd2*—are known to encode mitochondrial proteins (Chen et al., 2002; Gogos et al., 1999). Accordingly, we asked if there might be a larger subset of 22q11 genes localized to mitochondria, suggesting that combined diminished dosage might compromise mitochondrial function.

Mitochondrial dysfunction may contribute to a broad range of psychiatric disorders (Ben-Shachar, 2002; Bubber et al., 2004; Kung et al., 1999), perhaps due to the consequences of altered mitochondrial metabolism for survival of nerve cells and integrity of neural circuits. Synaptic transmission is metabolically demanding, and subtle alterations in mitochondrial integrity can alter brain function (Ben-Shachar et al., 2004). Synaptic mitochondria are also the site of several catabolic enzymes, including monoamine oxidases that rapidly inactivate neurotransmitters. Postmortem studies of schizophrenic brain tissue have associated changes in mitochondrial enzyme levels and activity with psychiatric disease (Bubber et al., 2004; Karry et al., 2004; Prabakaran et al., 2004). Moreover, the distribution of mitochondria is altered in schizophrenic brains (Kung et al., 1999). Thus, if a significant subset of 22q11 genes is associated with mitochondria, their diminished expression might compromise essential metabolic processes associated with synaptic transmission or other brain functions that are disrupted in psychiatric disorders associated with 22q11DS.

Accordingly, we evaluated potential mitochondrial association of genes found in the minimal 1.5 MB 22q11 minimal critical deleted region. We found six 22q11 proteins definitively localized to mitochondria, including neuronal mitochondria. Each is expressed at moderate to high levels in the CNS, reaches expression maxima during early postnatal life, and has apparently selective or specific expression in the olfactory bulb, cerebral cortex, basal ganglia and cerebellum. It is possible that diminished expression of one, some or all of these mitochondrial-localized 22q11 proteins (Meechan et al., 2006) contributes to mitochondrial dysfunction, including aberrant regulation of neuronal metabolism and synaptic signaling.

Materials and Methods

Informatics, cloning and expression of fusion proteins for putative mitochondrial proteins

We used two computational analysis algorithms: MitoProt (Claros, 1995) (<http://ihg.gsf.de/ihg/mitoprot.html>) and iPsort (Bannai et al., 2002) (<http://hc.ims.u-tokyo.ac.jp/iPSORT>) to identify potential mitochondrial proteins among the 22 mouse orthologues of human 22q11 genes known to be expressed in the brain (Maynard et al, 2003). For 9 putative mitochondrial proteins identified by these algorithms, the full open reading frame was cloned from either pooled mouse brain cDNA or an EST clone. A linker was added at the C-terminus of each full-length clone (removing the stop codon) with a restriction site in frame with pEGFP-N1 (Supplementary Table 1). Variants of these constructs (e.g. N-terminal and C-terminal deletions) were made by PCR amplifying reading frames

expressing specific fragments with linkers that add start codons and restriction sites to facilitate subcloning (Supplementary Table 1). All expression constructs were verified by sequencing. pCherry-Mito and pCherry-Golgi were generated by replacing the GFP portion of pEGFP-Mito and pEGFP-Golgi (Clontech, Mountain View, CA, USA) with the monomeric red fluorescent protein mCherry (gift of R. Tsien, Shaner et al., 2005), and a FLAG epitope (DYKDDDDK) added to the C-terminal end. pCherry-Peroxi was generated by adding a YKSKL peptide sequence to mCherry-Flag.

GFP fusion proteins were assayed by electroporating 3T3, L, or primary fibroblast (MEF) cells with a square-pulse electroporator (BTX-830, Harvard Apparatus, Holliston, MA, USA) and allowing cells to recover overnight, then replating into permanox chamber slides (Nalge Nunc, Rochester, NY, USA) for an additional 24 hours before fixation. Cells were fixed for 1 hour in 4% paraformaldehyde, and the GFP and Cherry signals were amplified using a rabbit anti-GFP (Invitrogen, Carlsbad, CA, USA) and purified mouse anti-FLAG (Sigma, St. Louis, MO, USA) antibodies, and Alexa 488 and 543 dye conjugated secondary antibodies (Invitrogen). All images were taken using approximately 1 μm optical sections on a Zeiss LSM-510 laser scanning confocal microscope.

3T3 and L (L-M^{tk-}) cells were obtained from ATCC (Manassas, VA). Primary fibroblasts (MEFs) were obtained by trypsinizing E14 embryos (from which the head and viscera had been removed) for 30 minutes, cleared of debris using a 40 μm mesh cell strainer (BD Falcon), and plated in DMEM. MEF cultures were used between 3 and 5 passages from original derivation.

In situ hybridization and quantitative PCR

For *in situ* hybridization, fragments of each transcript were cloned into pBluescript, then digoxigenin-labeled sense and antisense riboprobes were generated as described previously (Meechan et al., 2006). Cryostat sections from adult (age > 60 days) or P10 mice were prepared and hybridized using standard techniques. Sense control probes showed no significant labeling. Sections were imaged using a Wild Macrozoom video photomicroscope, or a Leica DMR video microscope. cDNA samples from whole brains dissected from embryos harvested from accurately timed pregnancies (morning of sperm plug=E0.5) were prepared from Trizol (Gibco)-extracted mRNA samples. Quantitative PCR analysis was performed as described previously (Meechan et al., 2006) using Taqman primers and the Applied Biosystems (ABI) qPCR platform. Analysis of mitochondrial gene expression in the Lgd1 mouse (Merscher et al., 2001) was performed by dissecting cortical hemispheres from appropriately aged postnatal animals, preparing cDNA samples as above, and analyzing expression levels using mitochondrial specific primers (Supplemental Table 2) with the Sybr Green analysis platform (ABI).

Antibody production and expression analysis

We generated three novel antibodies against 22q11 proteins. To produce each of these antibodies, two chickens were immunized with peptide sequences (Aves Labs, Tigard, OR, USA) representing these three 22q11 proteins: Mrpl40, KQEHMERDAIRS; T10, DKDTSRWETNTYEFTLQS; Zdhhc8, DEDEDKEDDFRAPLYKNVDVR. The resulting antisera were affinity purified, and antibodies were verified by western blotting against bacterially expressed fragments of each protein, as well as blocking by preabsorption with the immunogenic peptide prior to western blotting. T10 recognizes a single band close to the predicted molecular weight on western blots, and Mrpl40 identifies two bands, one at the predicted molecular weight of ~25 kD, and a second, larger band of unknown identity (~40 kD). Zdhhc8 antiserum recognized multiple protein bands, corresponding to multiple variants of the protein, as described below. We also used a rabbit polyclonal antiserum against Txnrd2 (#16841, Abcam, Cambridge, MA, USA); this antibody recognizes two bands in some tissues,

the larger of which is Txnrd2. Western blot analysis was performed as described previously (Meechan et al., 2006). Of these four antisera, only the Zdhhc8 antiserum proved useful for immunohistochemistry (see below).

Brain fractions for western blot analysis were made by homogenizing freshly dissected mouse brain tissue in extraction buffer [250 mM sucrose, 10 mM Tris pH 7.4, 1 mM EDTA, 0.05% protease inhibitor cocktail (Sigma)] on a motor-driven glass-teflon rotary dounce at approximately 1000 rpm for 15 strokes; large cellular fractions and debris were separated by centrifugation at 500g for 5 minutes. Crude mitochondrial fractions were prepared by centrifugation at 10,000 g for 10 minutes. These samples were sonicated to assess solubility (2 × 5 second pulses @ 50% power) or treated with detergent for 20 minutes, then re-centrifuged at 10,000 g for 10 minutes. Synaptosomes were prepared in a manner similar to Lau et al. (1996) by collecting a crude synaptosomal fraction by centrifugation at 10,000g for 10 minutes, suspending this pellet in a 300 mM sucrose buffer, collecting the interface from a 1.2 M sucrose step gradient (centrifuged at 100,000g in a SW28 rotor for 30 minutes), then re-purifying by collecting the pellet from a 0.8 M sucrose step gradient. Synaptosomal and free mitochondrial fractions were harvested from samples of adult cortex and subcortical forebrain including the basal ganglia and basal forebrain nuclei (Lai et al., 1976). Lysates were prepared as above, and centrifuged at 1100 × g for 5 minutes to remove nuclei and cell debris. Free mitochondria and synaptosomes were collected by harvesting the pellet and interface, respectively, of a 7.5%/13% Ficoll step gradient; synaptosomes were then lysed and synaptosomal mitochondria collected as the pellet of a second Ficoll step gradient.

Yeast two-hybrid analysis

Bait fragments for each of the six mitochondrial-localized proteins (Supplementary Table 1) were inserted into pGBK-T7 (Clontech), and used to transform an AH109 yeast reporter strain (Clontech). After checking constructs for auto-activation by plating yeast on -Trp/-His media, cells were transformed with either an adult mouse brain or E17 whole mouse embryo library (Clontech) and positive interactions detected by looking for growth on selective (-Leu/-Trp/-His) media. Positive clones were harvested, and the prey plasmid inserts were sequenced.

Cell death and metabolism assays

For analysis of the dose-dependent effects of Zdhhc8 overexpression, a construct was generated that contains a stringent form of the tetracycline inducible promoter (pTRE-Tight, Clontech) driving HA-tagged Zdhhc8, and a Tet-On-IRES-neo cassette inserted into the vector backbone. Linearized DNA for this construct was transfected into 3T3 cells, and a stable cell line was selected that expresses Zdhhc8 following the addition of doxycycline. To assess cell death, cells were induced with doxycycline, then incubated with the cell-impermeant dye Propidium Iodide (20 μM, Invitrogen) and the cell permeant dye Sybr Green (1X, Invitrogen) for 30 minutes in Optimem media with 4% Tet-Free FBS). Cells were washed in Optimem media and imaged live. To measure metabolic activity, cells were washed in Optimem media, and incubated for 2 hours with 0.5 mg/ml MTT (3-(4,5-Dimethylthiazol-2-yl)-2,5-diphenyltetrazolium bromide, Invitrogen) in Optimem media. Cells were washed twice with media, the formazan product was solubilized by adding 100 μl DMSO, and the reaction was quantified by measuring the absorbance at 570 nm in a microplate reader. We assessed co-expression of Bcl-2 by transfecting the stable Tet-Zdhhc8 cell line with a construct expressing a Flag-tagged Bcl2-IRES-Hygromycin and selecting for Hygromycin resistant cells; uniform expression of Bcl-2 was confirmed by immunostaining for the Flag epitope. Free-radical generation was blocked in cultured cells by the addition of 50 μM N-t-butyl-phenylnitron (PBN, Sigma).

Immunocytochemistry

Cryostat sections were prepared from aldehyde-perfused young adult mouse brains (age P21) and double-immunostained using standard protocols. Antibodies used were: Zdhhc8 polyclonal-1:500; Uqcrc1-1:200 (mouse, Invitrogen); Map2-1:1500 (mouse, Chemicon); Synaptophysin-1:1500 (mouse, Chemicon); GFAP-1:1000 (mouse, Chemicon); OMP 1:2000 (goat; Wako); Vglut1-1:1500 (guinea pig; Synaptic Systems), GABA-1:800 (rabbit, Sigma); GAD67-1:2000 (mouse, Chemicon); parvalbumin 1:4000 (rabbit, Swant, Bellinzona Switzerland). For detection, species-appropriate Alexafluor (Invitrogen) 488 and 546 secondary antibodies were used. Sections were imaged using a Zeiss LSM-510 laser scanning confocal microscope.

Results

Informatic Analysis of candidate mitochondrial 22q11 proteins

We used bioinformatic analysis to identify possible mitochondrial targeting motifs in the amino acid sequences of 22 22q11 proteins within the 1.5 minimal deletion region that are significantly expressed in the developing or mature mouse brain (Maynard et al., 2003). We used two computational analysis algorithms, MitoProt (Claros, 1995) and iPsort (Bannai et al., 2002) that probe putative N-terminal amino acid sequences, generally assumed to include a signal peptide important for subcellular targeting. Computational prediction of protein targeting is imprecise; therefore, it is not surprising that the two programs showed a low degree of consensus (Supplementary Table 3). Only one protein, Txnrd2, a known mitochondrial enzyme, was unambiguously identified as mitochondrial in human and mouse. We therefore used a lower threshold to identify additional mitochondrial candidates. We selected 22q11 proteins that showed at least a 70% probability of mitochondrial targeting assessed by MitoProt, or predicted to be mitochondrial by iPsort. Using these criteria, 9 proteins—Gnbl1, Mrpl40, Prodh, Rtn4r, Slc25a1, T10, Txnrd2, Ufd11, Zdhhc8—had N-terminal sequences with suggestive biophysical characteristics (iPsort, Mitoprot) or homology to known mitochondrial targeting motifs (iPsort) (Figure 1A).

Mitochondrial localization of a subset of 22q11 proteins

Bioinformatic predictive methods, especially with low comparison thresholds, are likely to produce false positives; accordingly, we evaluated directly whether any of the nine putative mitochondrial proteins are associated with mitochondria. We transiently transfected NIH-3T3 cells with constructs encoding fusion proteins of full coding sequence (minus the stop codon) for Gnbl1, Mrpl40, Prodh, Rtn4r, Slc25a1, T10, Txnrd2, Ufd11, and Zdhhc8, with EGFP added in frame to the C-terminus. Five fusion proteins (Mrpl40, Prodh, Slc25a1, T10, Txnrd2) were found in puncta, consistent with mitochondrial localization (Figure 1B). A sixth, Zdhhc8, appeared toxic to 3T3 cells when overexpressed (even briefly); but rapid examination of transiently transfected primary mouse embryonic fibroblasts (MEFS; 10 hours post-transfection) revealed that it, too, had punctate expression consistent with mitochondrial localization (Figure 1B, asterisk). The three remaining proteins showed localization inconsistent with mitochondria: Gnbl1, Rtn4r and Ufd11 were found in a uniform granular pattern throughout the cytoplasm, with no puncta consistent with mitochondrial labeling (Figure 1B). Thus, six 22q11 proteins, including two (Txnrd2 and Prodh) already assumed to be mitochondrial, appear localized to mitochondria.

To confirm these initial observations, we co-transfected the five putative mitochondrially-targeted 22q11 EGFP fusion proteins that were not cytotoxic when overexpressed with one of three fusion proteins with established subcellular targets: mitochondria, golgi, and a distinct punctate organelle, the peroxisome. We analyzed the sixth gene Zdhhc8, which causes rapid cell death when over-expressed, separately (see below). For the organelle-reporter constructs,

a monomeric red fluorescent protein (mCherry, gift of R. Tsien; Shaner et al., 2005), replaced EGFP as the reporter. The five putative mitochondrial proteins colocalized extensively with the mitochondrially targeted fusion protein (pCherry-mito), but showed minimal co-localization with golgi (pCherry-golgi) and peroxisome (pCherry-peroxisome) fusion proteins (Figure 2). In contrast, *Gnbl1*, *Rtn4r* and *Ufd1l* did not show co-localization with pCherry-mito (Supplemental Figure 1)

To determine whether the N-terminal targeting domains predicted by bioinformatics were responsible for mitochondrial localization of these five proteins, we produced EGFP fusion proteins using either the presumed N-terminal signal sequence, or an N-terminal fragment with the putative signal peptide removed (Figure 2; see also Supplemental Table 1). The N-terminal signal peptide sequence was sufficient for apparent mitochondrial localization for only two proteins: *Mprl40*, and *Prodh*. In contrast, the C-terminal fragment properly targeted *Slc25a1* and *T10*, and only full length *Txnrd2* localized to mitochondria. Thus, all five proteins are indeed mitochondrial; however, the domains that target each are apparently more variable than those predicted by the initial bioinformatics analysis.

To evaluate whether the *Zdhhc8* puncta were indeed mitochondrial, we used a polyclonal antibody generated to a region near the DHHC domain to circumvent the cytotoxicity that occurs when *Zdhhc8* fusion proteins are transfected into cell lines. In two fibroblast cell types, primary mouse embryonic fibroblasts (MEFS) and a mouse fibroblast cell line (L), *Zdhhc8* immunoreactivity was evident in distinct puncta, which co-localized very closely with *Uqcrc1*, an established mitochondrial protein, and a component of the mitochondrial complex III (Figure 3A,B). There is high homology (58% identity) between *Zdhhc8* and another *Zdhhc* family member, *Zdhhc5*, and both are expressed in L cells (data not shown). Nevertheless, our antibody only detects significant punctate labeling in presumed mitochondria, and not the cell membrane staining expected for *Zdhhc5* (Ohno et al., 2006).

CNS Expression of mitochondrially targeted 22q11 genes

To better define possible functions of the mitochondrial 22q11 proteins in the nervous system, we evaluated expression of each gene in the mature mouse brain by *in situ* hybridization. We focused upon three separate brain regions, the olfactory bulb and cerebellum, whose distinctive cytoarchitecture facilitates assessment of cell classes, as well as the cerebral cortex, which is thought to be the primary target of pathogenesis in psychiatric disorders associated with 22q11DS. All transcripts for apparent 22q11 mitochondrial genes are expressed in the olfactory bulb, neocortex and cerebellum (Figure 4). Two of the genes, the citrate transporter *Slc25a1* and thioreductase *Txnrd2* are expressed minimally, but apparently ubiquitously, throughout the brain. In addition, *Slc25a1* is highly expressed in a subset of large cells in the globus pallidus (Figure 4, inset). *Prodh* and *Zdhhc8* are expressed in the bulb, neocortex, and cerebellum; however, there are discontinuities in apparent levels in distinct cell classes. In both bulb and cerebellum, *Zdhhc8* and *Prodh* appear more robustly in projection neurons: mitral cells and Purkinje cells, respectively. *T10* and *Mprl40* have more circumscribed and complex expression patterns. Both are elevated in mitral cells and minimally (*T10*) or moderately (*Mprl40*) expressed in bulb interneurons. In the cortex, *T10* is restricted to the upper portion of layer 5 and *Mprl40* is enhanced in apparent neurons at the boundary of cortical layers 4 and 5. In the cerebellum, *T10* is excluded from Purkinje cells, but expressed in granule cells, while *Mprl40* is enhanced in Purkinje cells. Accordingly, all six mitochondrial-localized 22q11 genes are expressed in the adult olfactory bulb, cerebral cortex and cerebellum in distinct patterns, and 4/6 (*Prodh2*, *Zdhhc8*, *T10* and *Mprl40*) apparently have elevated expression in several classes of projection neurons.

We next asked when these expression differences are established during development—particularly during the postnatal period when the majority of synapses are formed in the cortex

and other brain regions (Knaus et al., 1986; Pomeroy et al., 1990). Quantitative PCR indicates that all of the 22q11 mitochondrial genes are dynamically expressed. They reach peak expression levels in the brain between P0 and P21, and decline either slightly or substantially thereafter (Figure 5, left). To determine whether these temporal changes correspond to dynamic expression patterns, we localized 4/6 genes whose expression is distinct in the adult: *Prodh*, *Zdhhc8*, *T10* and *Mrpl40* (Figure 5, right) in the early postnatal brain (P10), when expression levels are highest. In the olfactory bulb and cortex, the adult expression pattern for each gene is in place by P10, including expression in mitral cells, apparent cortical pyramidal cells, and Purkinje cells. In addition, for *Zdhhc8*, *T10* and *Mrpl40* there is robust expression in a small population of cells at the boundary of layer 6 and the developing white matter. These cells are most likely the remnants of the cortical subplate, which in rodents begins to regress at this time. In the cerebellum, Purkinje cell expression is established by P10 for *Prodh*, *Zdhhc8* and *Mrpl40*, but not for *T10*, which is absent from these cells in the adult. All four genes, however, are also expressed in the transient external granule cell layer as well as in the nascent internal granule cell layer (Figure 5, right, bottom row). Thus, the adult pattern of mitochondrial 22q11 genes is mostly in place by P10, when expression levels are near maximal. There is additional expression, however, in transient cellular zones—the cortical subplate and cerebellar external granule cell layer—during early postnatal development.

22q11 proteins are found in brain mitochondria and synapses

To assess the native subcellular localization of 22q11 mitochondrial genes that are expressed in the cortex and other brain regions (i.e. without overexpression of epitope-tagged constructs), we first asked whether a subset was enriched in brain mitochondria. We analyzed four proteins (*Mrpl40*, *T10*, *Txnrd2*, and *Zdhhc8*) using western blots of brain lysate fractions enriched by differential centrifugation. We found robust expression defined by a single dominant band or doublet of appropriate molecular weight for several mitochondrial 22q11 proteins, as well as two known mitochondrial proteins (Cytochrome C and *Uqcrc1*) in the 10k fraction, which is enriched for mitochondria (Figure 6).

Zdhhc8 expression was somewhat more complex; a predominant band was observed around 40 kD, approximately half the predicted molecular weight of the unprocessed protein (~80 kD) was seen in all fractions; however, two less dominant bands were observed around 70–75 kD. The largest band, around 75 kD, only was observed in unfractionated samples, and the next largest band, around 70 kD, was enriched in all fractions predicted to contain mitochondria. The dominant 40 kD band does not appear to be predicted by multiple transcriptional forms identified in human tissues by previous studies (Mukai et al., 2004). Pre-absorbing the antiserum with the specific *Zdhhc8* immunogenic peptide abolishes detection of all of these bands.

To further establish mitochondrial and neuronal localization of these 22q11 proteins, we fractionated the brain lysates in several ways: we lysed mitochondria by sonication to determine whether the protein could be released into a soluble fraction. *Mrpl40*, *T10*, *Txnrd2*, and both the 40 and 70 kD forms of *Zdhhc8* are readily released into the soluble fraction after mitochondrial lysis, in parallel with Cytochrome C and *Uqcrc1* (Figure 6). Second, we evaluated enrichment in distinct neuronal compartments using a sucrose step gradient to enrich for synaptosomes (Lau et al., 1996). *Mrpl40*, *T10*, *Txnrd2*, and both the 40 and 70 kD *Zdhhc8* isoforms are substantially enriched in the step gradient pellet containing synaptosomes, verified by synaptophysin expression, while the interface (synaptosome poor) shows little immunoreactivity for any 22q11 mitochondrial protein, established mitochondrial protein or synaptophysin (Figure 6).

To further refine this subcellular localization, we prepared lysates from adult cerebral cortex and the subcortical forebrain (including the thalamus and basal ganglia). From each lysate, we

isolated a soluble fraction, a free mitochondrial fraction (enriched for mitochondria from the cell body, but excluding those in synaptosomes), and a synaptosomal mitochondrial fraction (Lai et al., 1976). Txnrd2 and the 70 kD Zdhhc8 isoform were enriched in both synaptosomal and free mitochondrial populations. In contrast, the 40 kD isoform of Zdhhc8 was found in the soluble fraction, although it was also observed in the free mitochondrial fractions at a lower level (Figure 7A).

Zdhhc8 is expressed in presynaptic processes

We next asked whether the mitochondrial proteins have a distinctive subcellular expression pattern in neural tissue. Of the antibodies commercially available, or produced for this study, only Zdhhc8, which has been independently identified as a schizophrenia risk gene in non-22q11 deleted individuals (Liu et al., 2002b; Mukai et al., 2004), yielded a reliable reagent for immunohistochemical staining. We confirmed immunohistochemical specificity of our antibody by staining adult brain sections with pre-immune serum as well as antiserum pre-absorbed with the immunogenic peptide. The Zdhhc8 antiserum yielded a punctate pattern of staining in areas known to consist primarily of neuropil; however the pre-immune and pre-absorbed sera produced no detectable signal (Supplemental Figure 2).

To better resolve whether Zdhhc8 is preferentially associated with specific cellular compartments—particularly pre-synaptic processes—we assessed coincident expression of Zdhhc8 and Map2 (dendrites), synaptophysin (synapses) and glial fibrillary acidic protein (GFAP, astrocytes and processes) in the olfactory bulb, neocortex and cerebellum since each region has distinct cell body-rich, neuropil-rich and glial compartments (Figure 7B). Zdhhc8 is excluded from or minimally localized in neuronal cell bodies, dendrites, or glial cells and processes. In contrast, there is consistent coincident expression of Zdhhc8 and synaptophysin in neuropil-rich regions of the olfactory bulb, cerebellum, and neocortex. In all locations, Zdhhc8 is often seen in distinct ring-like structures, coincident with synaptophysin, presumably in presynaptic endings (Figure 7B).

Zdhhc8 is not seen in all profiles labeled by synaptophysin, suggesting that this protein may be selectively expressed in distinct classes of synapses. Accordingly, we asked whether Zdhhc8 is preferentially associated with inhibitory versus excitatory synapses. We focused on the olfactory bulb, because of its well-defined cytoarchitecture; however our observations in the bulb parallel those in the neocortex, cerebellum, and hippocampus (data not shown). There was no absolute coincidence of Zdhhc8 with any markers that distinguish excitatory (OMP, for primary olfactory afferents, which are glutamatergic, or the vesicular glutamate transporter 1—VGLUT1—for glutamatergic terminals of CNS neurons), or various classes of inhibitory neuropil elements (GABA, GAD67, parvalbumin in various OB interneurons) in olfactory glomeruli (Figure 7C). Nevertheless, there is more frequent co-localization in glutamatergic, presumably excitatory terminals (i.e. those co-labeled for OMP or Vglut1). Little coincidence was seen between Zdhhc8 and cells or processes expressing Parvalbumin. Apparently Zdhhc8 is associated with molecularly distinct subsets of excitatory and, to a much lesser extent, inhibitory presynaptic processes.

Zdhhc8 dosage regulates cell survival and death

We next asked whether the 22q11 mitochondrial proteins directly influence cellular functions associated with mitochondria. We focused on Zdhhc8, since our initial cellular evaluation indicated that over-expression of Zdhhc8 in cell lines and primary cells is toxic. Similar over-expression of the other five mitochondrial proteins does not yield observable phenotypes in cell lines. This suggests that cells may be sensitive to Zdhhc8 dosage, perhaps due to disrupted mitochondrial function. Indeed, even modest over-expression of Zdhhc8 for 16 hours using a tetracycline inducible promoter in 3T3 cells causes mitochondria to become dysmorphic

(Figure 8A). Following longer induced expression, or expression driven by a stronger CMV promoter, only highly dysmorphic cells or cellular debris are observed in a number of cell types including primary fibroblasts (Figure 8B, C). Mitochondrial integrity is apparently disrupted since co-expressed pCherry-mito, usually limited to mitochondrial puncta, appears diffuse and cytosolic (Figure 8B, C). To further assess the dose-dependence of Zdhhc8-induced cell death, we produced a stable cell line expressing Zdhhc8 under the control of a stringent tetracycline inducible promoter (pTRE-tight). When increasing amounts of doxycycline are added to induce Zdhhc8 expression, cell death (measured by nuclear staining of live cultures by the membrane-impermeant fluorescent dye Propidium Iodide) the proportion of dead cells increased with dosage, reaching 44.5% after 18 hours of exposure at the highest measured dose (Figure 8D, see also 8M).

To evaluate whether a specific domain of Zdhhc8 mediates this dosage-dependent toxicity, we expressed Zdhhc8 fragment-GFP fusion proteins in 3T3 cells (Figure 8E). The N-terminus (aa1-87, containing the putative signaling peptide) is neither sufficient for mitochondrial targeting nor toxic (Figure 8F). A C-terminal fragment, containing 2/3rds of Zdhhc8, but lacking the DHHC domain (aa272-762) was neither toxic, nor localized to mitochondria (Figure 8G). In contrast, a fragment lacking only the putative N-terminal signal peptide (aa42-762) localized to mitochondria (Figure 8H), and was toxic to a similar degree as full-length Zdhhc8. To assess whether reduced toxicity was a function of mislocalization, we attached the same mitochondria targeting signal used in our pCherry-Mito construct to the non-toxic C-terminal fragment (aa327-762), excluding the DHHC domain. The expressed protein was localized to mitochondria (Figure 8I), but no toxicity was evident, even after several days in culture. In contrast, the N-terminal fragment that includes the DHHC domain (aa1-327), was still toxic and appears localized to the remnants of mitochondria in dysmorphic cells (Figure 8J). Thus, both the mitochondrial localization and toxicity of Zdhhc8 appear to be functions of the N-terminal portion of the protein (aa87-272) that excludes the N-terminus itself, but includes the DHHC zinc finger domain.

To further evaluate the dose-dependence of apparent Zdhhc8 mitochondrial function, we assessed cell viability of the doxycycline inducible stable Zdhhc8 expressing cell line by measuring mitochondrial metabolism of MTT (3-(4,5-Dimethylthiazol-2-yl)-2,5-diphenyltetrazolium bromide) a substrate for mitochondrial succinic dehydrogenase that is only metabolized in functionally intact mitochondria, at 16, 20, and 24 hours after induction by doxycycline. MTT metabolism is diminished in a dose dependent manner after 20 or 24 hours (Figure 8K). However, we also found that at 16 hours, intermediate dosages of doxycycline produce an apparently transient increase in MTT metabolism (Figure 8K). This transient rise in MTT metabolism could be due to several factors, such as increased mitochondrial activity, proliferation in response to cellular stress, or the creation of free radicals. The latter appears most likely, as this increase is apparently quenched by the addition of N-t-butyl-phenylnitron (PBN), a spin-trap compound that quenches many free radicals (Figure 8L). In general, the decreased metabolic activity at higher dosages of doxycycline appears to correspond to the onset of cell death; by 18h after a high dose of doxycycline, a significant proportion (44.5%) of cells are dead, and statistically significant levels of death are measurable at 18 hours for all dosages that show substantial decreases in MTT activity by 20 hours.

A critical test of the mitochondrial function of Zdhhc8 is whether Zdhhc8 induced cell death engages the apoptotic pathway, which depends ultimately upon mitochondrial integrity. Zdhhc8 induced cell death is likely apoptotic. Co-expression of the anti-apoptotic mitochondrial protein Bcl-2 significantly reduces the level of dead cells following high-dose doxycycline treatment: from 44.5% (Figure 8M) to approximately 2.5% (Figure 8N). Similarly, the addition of the free radical inhibitor PBN, which should minimize oxidative stress that can

lead to mitochondrial initiation of apoptosis, also reduces the proportion of dead cells (Figure 8O). Thus, one of the 22q11 mitochondrial genes, *Zdhhc8*, regulates mitochondrial metabolism as well as mitochondrial-regulated cell survival and cell death in a dosage-dependent manner.

Zdhhc8 interacts with mitochondrial Complex III

The rapid onset of cell death following *Zdhhc8* overexpression, and attenuation of death by Bcl-2 overexpression and free radical quenching, suggests that elevated *Zdhhc8* dosage directly influences mitochondrial metabolic mechanisms that ultimately regulate cell survival and death. Accordingly, we asked whether *Zdhhc8* interacts with proteins that might influence mitochondrial metabolism using a yeast 2-hybrid screen of an adult mouse brain library. We produced two full-length baits for the two separate functional domains of *Zdhhc8* (the N-terminal DHHC zinc-finger domain, flanked by transmembrane domains, and a unique C-terminal domain). The N-terminal DHHC zinc finger domain produced numerous artifactual hits: short fragments that contained fusions to non-coding sequences. However, the unique C-terminal domain yielded 10 positive colonies from the adult brain library, all 10 of which represented fragments of *Uqcrc1*, (ubiquinol cytochrome reductase 1), core protein 1 of mitochondrial core complex III. We also screened additional 22q11 mitochondrial genes—*Mrpl40*, *Prodh*, *Slc25a1*, and *T10*; however, we found no evidence of significant protein-protein interactions for these using the two-hybrid assay

To further clarify the *Zdhhc8/Uqcrc1* interaction, we produced a set of deletion constructs that contain fragments of both the C-terminal domain of *Zdhhc8*, and fragments of *Uqcrc1*. Using these constructs, we mapped the interaction domain to an approximately 100 amino acid region of *Uqcrc1* and a similar sized region of *Zdhhc8* (Figure 9A). We further analyzed the possible physical proximity of these two proteins by assessing their solubility from mitochondrial membranes (Ko et al., 2003). *Zdhhc8* and *Uqcrc1* appear to have similar solubility. They are released into solution from a brain mitochondrial fraction by similar concentrations of various detergents, suggesting that they occupy a similar mitochondrial compartment (Figure 9B). Attempts to co-immunoprecipitate *Zdhhc8* from native tissues (whole brain and fibroblast cultures) were unsuccessful. Complex III is a large, multi-protein complex, which may have up to 30 or 40 associated proteins (Schilling et al., 2006). Isolating intact Complex III is apparently quite challenging; even fairly mild solubilization and detergent conditions appear to dissociate some proteins from the complex, changing its function and characteristics (Wittig et al., 2007) Co-immunoprecipitation using full-length overexpressed *Zdhhc8* fusion protein was not possible due to the toxicity of the protein product.

Despite the biochemical difficulties for co-precipitation, tissue co-localization supports the possibility of interaction between *Zdhhc8* and *Uqcrc1*. *In vivo*, *Zdhhc8* and *Uqcrc1* are coincidentally expressed in the neuropil of the olfactory bulb, neocortex and cerebellum. The two proteins are co-localized in numerous puncta in neuropil of all three regions (Figure 9C, left hand panels). This coincident expression is not exclusive to either protein (not all *Zdhhc8* puncta are also labeled for *Uqcrc1*, nor are all *Uqcrc1* puncta labeled for *Zdhhc8*); however, it is limited to neuropil-rich regions. The primary expression of both *Zdhhc8* and *Uqcrc1* is in clusters of ring-like structures within the neuropil (insets, Figure 9D, right hand panels), similar to the co-localization of *Zdhhc8* and synaptophysin as well as *Vglut1*. We do not see *Zdhhc8* in cell bodies, and *Uqcrc1* is only occasionally detected in cell bodies (insets, Figure 9, right hand panels). Thus, the coincident expression of *Zdhhc8* and *Uqcrc1* in subsets of apparent synaptic endings is consistent with a potential biochemical interaction between these two mitochondrial proteins.

Mitochondrial Core Complex III transcripts are altered in a mouse model of 22q11 deletion

The significant number of mitochondrial 22q11 genes, as well as the clear functional influence of *Zdhhc8* on mitochondrial function suggests that 22q11 deletion, which leads to diminished dosage of these 6 genes as well as 16 additional genes in the brain, might influence mitochondrial integrity. To begin to address this issue, we assessed the expression of several mitochondrial transcripts in cortical samples from Lgdel mice on P0, when mitochondrial genes are normally at an expression maximum, and at P40 when normal levels of these genes have declined significantly. We have shown previously that expression of multiple 22q11 genes is reduced by roughly 50% in all tissues and ages thus far examined (Meechan et al., 2006). Thus, it is unsurprising that *Zdhhc8* expression is significantly reduced by 50% in cortical samples ($P < 0.001$) at both P0 and P40. In contrast, a non-mitochondrial transcript expressed in the cortex (*Gfap*) is expressed at normal levels in both P0 and P40 Lgdel mice (Figure 10, $P > 0.8$). We measured expression of eight independent mitochondrial transcripts (Figure 10), including six associated with Complexes I–IV. These transcripts were all from different chromosomal loci, including one (*Mtco1*) expressed from the mitochondrial genome. Within this set of mitochondrial transcripts, there is a general trend towards increased levels of expression at P0, although only transcripts from Complex III (*Uqcrc1*, *Uqcrc2*) reach statistical significance ($P < 0.005$ and $P < 0.05$, respectively). This increased expression diminishes to normal levels in maturity; at P40, no mitochondrial transcripts other than *Zdhhc8* are significantly different in Lgdel and wild type cortices.

Discussion

A significant subset of 22q11 genes expressed in the developing or mature brain—6/22 or nearly 30%—are restricted to a single organelle, the mitochondrion. Distinct expression patterns and dynamic expression levels of these genes in the developing and adult brain suggest they contribute to construction and maintenance of neural circuits, particularly for projection neurons. Following 22q11 deletion, diminished expression of any or all of these genes—particularly during early postnatal development—may compromise brain mitochondrial function, a fundamental regulator of metabolism and homeostasis previously suggested as a pathogenic target in schizophrenia and other psychiatric disorders associated with 22q11DS. Indeed, our results show that dosage change of at least one of these genes, *Zdhhc8*, can specifically disrupt mitochondrial function. Finally, expression levels of additional mitochondrial genes change in the developing but not the adult brain after 22q11 deletion. Thus, altered dosage of the six 22q11 mitochondrial genes particularly during early postnatal life may contribute to increased vulnerability for psychiatric disorders in 22q11DS patients.

Mitochondrial functions for a subset of 22q11 genes

Our informatics analysis identified nine 22q11 genes as potential mitochondrial proteins; however, only six are localized to mitochondria. Among the six confirmed 22q11 mitochondrial proteins, four are most likely involved in mitochondrial metabolism, either regulating levels of small molecule metabolites: *Prodh* (Gogos et al., 1999), *Txnrd2* (Chen et al., 2002), *Slc25a1* (Kaplan et al., 1995), or facilitating expression from the mitochondrial genome: *Mrpl40* (Accardi et al., 2004). Adult 22q11 DS patients have hyperprolinemia (Raux et al., 2007), indicating that the metabolic function of *PRODH* is compromised, presumably due to diminished dosage. *Txnrd2* has been analyzed previously in mammalian cells (Chen et al., 2006), and its role in reducing mitochondrial thioredoxin appears to be essential for preventing cell death. For the remaining four genes, two—*Slc25a1* and *Mrpl40*—have been assumed to be mitochondrial based on previous observations of yeast homologues (Accardi et al., 2004; Kaplan et al., 1995); however, they have not been directly assessed in mammalian cells. Thus, our data confirms or clarifies several other observations of apparent mitochondrial

function collected for mammalian 22q11 genes or their homologues in non-mammalian species.

The function of the remaining mitochondrial genes, *T10* and *Zdhhc8*, has been even less well characterized prior to our study. *T10*'s cellular localization and physiological properties have not been previously determined, and the inferred amino acid sequence gives no substantial clues to its potential function. *Zdhhc8* has been previously suggested to be in the golgi (Mukai et al., 2004; Ohno et al., 2006), and assumed to be a palmitoyl-transferase (Fukata et al., 2004; Mukai et al., 2004) based upon homology to other *Zdhhc* family members. The localization of *Zdhhc8* to mitochondria is unexpected since palmitoylation, like most post-translational protein modifications, is generally assumed to occur in the golgi and endoplasmic reticulum. Recent studies in yeast suggest a role for mitochondria in palmitoylation of at least one protein target (Wang et al., 2006); however, this role is still poorly defined. The mitochondrial localization of *Zdhhc8*, its mitochondrial-dependent cytotoxicity, and its apparent interaction with *Uqcrc1*, is inconsistent with its presumed activity as a palmitoyl-transferase. Thus our results provide novel insight into the potential function of two 22q11 proteins.

Additional insight into *Zdhhc8*'s possible functions may be gained by considering this protein in the context of *Uqcrc1*—which our data suggests may interact with *Zdhhc8* in mitochondria—in a range of psychiatric and cognitive disorders associated with 22q11DS. *Uqcrc1* is decreased in schizophrenic brains (Prabakaran et al., 2004) and increased in mood disorders (Johnston-Wilson et al., 2000) as well as a mouse model of Rett syndrome (Kriaucionis et al., 2006). Furthermore *Uqcrc1* expression levels influence the activity of mitochondrial complex III (Johnston-Wilson et al., 2000). Reduced expression of *Zdhhc8* in the mouse model of 22q11 deletion (Meechan et al., 2006) may release *Uqcrc1* from some as-yet undefined modulatory influence of its binding partner, perhaps leading to aberrant expression, electron transport and bioenergetic function. Thus, increased expression of *Uqcrc1* and other complex III components in the Lgdel cortex during early postnatal life reported here may indicate altered complex III activity. A preliminary analysis of metabolic activity in mitochondrial extracts from Lgdel mouse brains using the JC-1 redox-sensitive dye did not detect significant alteration in mitochondrial metabolism. The measurement error, however, is fairly high (>20%), and heterogeneity may mask changes if 22q11 mitochondrial proteins are found in subsets of brain mitochondria. Furthermore, increased expression levels of Complex III transcripts we report here may be compensatory: altered expression of mitochondrial proteins or increased total numbers of mitochondria in the Lgdel mouse might rescue some aspects of mitochondrial dysfunction.

Zdhhc8, cell death and mitochondrial function

We found that cell survival is sensitive to *Zdhhc8* dosage; however, it is not clear what mechanism underlies *Zdhhc8* toxicity. The death-promoting activity is most likely independent of the interaction with *Uqcrc1*; N-terminal fragments that do not contain the *Uqcrc1* binding domain defined by our yeast-two-hybrid assays are sufficient to cause rapid cell death. This effect seems specific to the *Dhhc* domain of *Zdhhc8*, rather than mitochondrial overexpression since a *Zdhhc8* fragment without the mitochondrial localization or *Dhhc* domain is not toxic. The cell death we observe is most likely apoptotic, and thus more likely to involve mitochondrial dysfunction. Indeed, *Bcl-2*, which normally prevents initiation of apoptosis via release of cytochrome C from mitochondria in response to cellular stress, rescues *Zdhhc8* cytotoxicity. At least one other *Zdhhc* family member may promote apoptosis. *Zdhhc16* (also known as *Aph2*) has a direct protein-protein interaction with *c-Abl*, and this interaction promotes apoptosis (Li et al., 2002). A screen for genes that modulate cell cycle arrest following irradiation induced DNA damage identified *Zdhhc8* as being required for modulating the

normal G₀/G₁ and G₂/M checkpoints (Sudo et al., 2007). Thus, some form of cell signaling via members of the *Zdhhc* family, perhaps modulated by the N-terminal/ *Dhhc* domain, may modulate aspects of cell cycle, cell survival, and/or death. We have analyzed mitochondrial-mediated toxicity when *Zdhhc8* was over-, rather than under-expressed (as would be expected following 22q11 deletion). The direction of expression change is opposite that in 22q11 deletion; nevertheless, our results demonstrate *Zdhhc8* dosage sensitivity. Some individuals have been described with 22q11 duplications, and their phenotypes overlap with those associated with 22q11DS (Portnoi et al., 2005). Such individuals presumably have increased levels of *Zdhhc8*, perhaps leading to disrupted mitochondrial function similar to those observed in our overexpression studies.

Brain expression and synaptic localization of 22q11 mitochondrial proteins

We found that six 22q11 proteins localized to mitochondria are expressed in the developing and adult brain, and enriched in brain synapses; nevertheless, we have not yet unequivocally established their biological function. Four mitochondrial genes, *Txnrd2*, *Prodh*, *Zdhhc8*, and *Mrpl40* are ubiquitously expressed in the brain; however *Prodh* and *Zdhhc8* appear most robust. They are seen in subsets of apparent projection neurons as well as interneurons in the olfactory bulb, neocortex, and cerebellum. The apparent ubiquitous expression of *Prodh* and *Zdhhc8* reaches peak levels during early postnatal life. Accordingly, diminished dosage in 22q11DS may have widespread consequences for circuit development in the cortex and other brain regions at this distinct point in early brain development (Meechan et al., 2006). The remaining genes may influence mitochondrial integrity in neurons with distinct (and possibly increased) metabolic demands reflecting size, connectivity, and levels of activity. *Mrpl40* appears more selectively, but not exclusively, associated with projection neurons in the bulb, cortex, and cerebellum. Two transcripts have even more limited expression patterns consistent with this suggestion: *Slc25a1*, though modestly expressed in all regions, is selectively expressed at high levels in large globus pallidus neurons, while *T10* is seen primarily in apparent pyramidal cells of neocortical layer 5. It is easy to imagine that high metabolic demand—for tonic inhibitory activity of globus pallidus projection neurons, or maintenance of long cortico-subcortical axons for layer V neurons—might require modulation of mitochondrial function, or a significantly increased number of specialized mitochondria that express these two proteins.

At least one 22q11 mitochondrial protein, *Zdhhc8*, is found primarily in apparent presynaptic processes. Nevertheless, *Zdhhc8* is not consistently associated with a singular class of presynaptic ending. *Zdhhc8* expression coincides most frequently with presumed glutamatergic profiles; nevertheless, expression is less frequently observed in at least two subtypes of GABAergic synaptic endings—those labeled for the transmitter GABA and the synthetic enzyme GAD67. Given the widespread expression of *Zdhhc8* in a variety of neuron classes, this diversity is not surprising. Nevertheless, the apparent preference for *Zdhhc8* in glutamatergic versus GABAergic processes indicates an enhanced role for *Zdhhc8* in excitatory synaptic transmission. These hypotheses remain to be tested; however, such normal functions for 22q11 mitochondrial proteins, if disrupted by diminished dosage and altered activity, could lead to synaptic changes currently implicated in pathogenesis of schizophrenia and other psychiatric disorders (Winterer et al., 2004). These include changes in activity dependent plasticity, process and synapse growth, cell survival and death—all of which depend upon trophic signaling, regulation of metabolic integrity, and modulation of mitochondrial function particularly during early post-natal life when the 22q11 mitochondrial genes are maximally expressed.

Mitochondria and multigenic mechanisms in 22q11DS cognitive disorders

Our observations suggest that mitochondrial function, altered by diminished dosage of mitochondrial 22q11 proteins from the 1.5 Mb deletion region, may be significant for

pathogenesis of psychiatric disorders seen in 22q11DS. Of the six 22q11 mitochondrial genes, *PRODH* and *ZDHHC8*, have SNPs robustly associated with schizophrenia, the psychiatric disorder whose association with 22q11DS has been most extensively evaluated (Liu et al., 2002a; Liu et al., 2002b). In addition *T10* has SNPs associated at a somewhat less robust level (Liu et al., 2002a), and *TXNRD2* has polymorphisms associated with a shared upstream promoter for the non-mitochondrial gene *Comt*. Additional observations implicate mitochondrial 22q11 genes in cognitive function: both *Prodh* and *Zdhhc8* yield behavioral anomalies when deleted homozygously in mice (Gogos et al., 1999; Mukai et al., 2004; Paterlini et al., 2005). In addition, *TXNRD2* is apparently elevated in schizophrenic brain samples (Prabakaran et al., 2004). The coincident expression and function of these 22q11 proteins in mitochondria may lead to a “convergence” of dysfunction when expression is diminished by a 22q11 deletion. Dosage changes—likely to be at least 50% of normal levels (Meechan et al., 2006)—might disrupt mitochondria by compromising stoichiometric or steric requirements for mitochondrial protein complexes. Thus, altered dosage of any one of these 22q11 genes may affect the function of a common organelle—the mitochondria—and cause developmental or functional consequences, including altered synaptic development or function that could contribute to increased vulnerability for psychopathology in 22q11DS.

Supplementary Material

Refer to Web version on PubMed Central for supplementary material.

Acknowledgements

NICHD (HD42182) and a NARSAD independent investigator award to A-S.L. supported this work, as did a NARSAD young investigator award to T.M., and a Silvio M. Conte Research for Mental Disorders Award to J.L. (MH64065). D.M. was a fellow of the UNC Developmental Biology Training Program (HD46369). Confocal microscopy and RNA expression analysis utilized UNC Neuroscience Center core facilities (NS031768).

References

- Accardi R, Oxelmark E, Jauniaux N, de Pinto V, Marchini A, Tommasino M. High levels of the mitochondrial large ribosomal subunit protein 40 prevent loss of mitochondrial DNA in null *mmf1* *Saccharomyces cerevisiae* cells. *Yeast* 2004;21:539–548. [PubMed: 15164357]
- Bannai H, Tamada Y, Maruyama O, Nakai K, Miyano S. Extensive feature detection of N-terminal protein sorting signals. *Bioinformatics* 2002;18:298–305. [PubMed: 11847077]
- Bassett AS, Chow EW. 22q11 deletion syndrome: a genetic subtype of schizophrenia. *Biol Psychiatry* 1999;46:882–891. [PubMed: 10509171]
- Ben-Shachar D. Mitochondrial dysfunction in schizophrenia: a possible linkage to dopamine. *J Neurochem* 2002;83:1241–1251. [PubMed: 12472879]
- Ben-Shachar D, Laifenfeld D. Mitochondria, synaptic plasticity, and schizophrenia. *Int Rev Neurobiol* 2004;59:273–296. [PubMed: 15006492]
- Bubber P, Tang J, Haroutunian V, Xu H, Davis KL, Blass JP, Gibson GE. Mitochondrial enzymes in schizophrenia. *J Mol Neurosci* 2004;24:315–321. [PubMed: 15456945]
- Chen WY, Shi YY, Zheng YL, Zhao XZ, Zhang GJ, Chen SQ, Yang PD, He L. Case-control study and transmission disequilibrium test provide consistent evidence for association between schizophrenia and genetic variation in the 22q11 gene *ZDHHC8*. *Hum Mol Genet* 2004;13:2991–2995. [PubMed: 15489219]
- Chen Y, Cai J, Murphy TJ, Jones DP. Overexpressed human mitochondrial thioredoxin confers resistance to oxidant-induced apoptosis in human osteosarcoma cells. *J Biol Chem* 2002;277:33242–33248. [PubMed: 12032145]
- Chen Y, Yu M, Jones DP, Greenamyre JT, Cai J. Protection against oxidant-induced apoptosis by mitochondrial thioredoxin in SH-SY5Y neuroblastoma cells. *Toxicol Appl Pharmacol* 2006;216:256–262. [PubMed: 16797630]

- Claros MG. MitoProt, a Macintosh application for studying mitochondrial proteins. *Comput Appl Biosci* 1995;11:441–447. [PubMed: 8521054]
- Fukata M, Fukata Y, Adesnik H, Nicoll RA, Bredt DS. Identification of PSD-95 palmitoylating enzymes. *Neuron* 2004;44:987–996. [PubMed: 15603741]
- Gogos JA, Santha M, Takacs Z, Beck KD, Luine V, Lucas LR, Nadler JV, Karayiorgou M. The gene encoding proline dehydrogenase modulates sensorimotor gating in mice. *Nat Genet* 1999;21:434–439. [PubMed: 10192398]
- Jerome LA, Papaioannou VE. DiGeorge syndrome phenotype in mice mutant for the T-box gene, *Tbx1*. *Nat Genet* 2001;27:286–291. [PubMed: 11242110]
- Johnston-Wilson NL, Sims CD, Hofmann JP, Anderson L, Shore AD, Torrey EF, Yolken RH. Disease-specific alterations in frontal cortex brain proteins in schizophrenia, bipolar disorder, and major depressive disorder. The Stanley Neuropathology Consortium. *Mol Psychiatry* 2000;5:142–149. [PubMed: 10822341]
- Kaplan RS, Mayor JA, Gremse DA, Wood DO. High level expression and characterization of the mitochondrial citrate transport protein from the yeast *Saccharomyces cerevisiae*. *J Biol Chem* 1995;270:4108–4114. [PubMed: 7876161]
- Karry R, Klein E, Ben Shachar D. Mitochondrial complex I subunits expression is altered in schizophrenia: a postmortem study. *Biol Psychiatry* 2004;55:676–684. [PubMed: 15038995]
- Knaus P, Betz H, Rehm H. Expression of synaptophysin during postnatal development of the mouse brain. *J Neurochem* 1986;47:1302–1304. [PubMed: 3091767]
- Ko YH, Delannoy M, Hullihen J, Chiu W, Pedersen PL. Mitochondrial ATP synthasome. Cristae-enriched membranes and a multiwell detergent screening assay yield dispersed single complexes containing the ATP synthase and carriers for Pi and ADP/ATP. *J Biol Chem* 2003;278:12305–12309. [PubMed: 12560333]
- Kriaucionis S, Paterson A, Curtis J, Guy J, Macleod N, Bird A. Gene expression analysis exposes mitochondrial abnormalities in a mouse model of Rett syndrome. *Mol Cell Biol* 2006;26:5033–5042. [PubMed: 16782889]
- Kung L, Roberts RC. Mitochondrial pathology in human schizophrenic striatum: a postmortem ultrastructural study. *Synapse* 1999;31:67–75. [PubMed: 10025685]
- Lai JC, Clark JB. Preparation and properties of mitochondria derived from synaptosomes. *Biochem J* 1976;154:423–432. [PubMed: 938457]
- Lau CO, Ng FH, Khoo HE, Yuen R, Tan CH. Inhibition of sodium-dependent uptake processes in purified rat brain synaptosomes by Lophozozymus pictor toxin and palytoxin. *Neurochem Int* 1996;28:385–390. [PubMed: 8740445]
- Li B, Cong F, Tan CP, Wang SX, Goff SP. Aph2, a protein with a zf-DHHC motif, interacts with c-Abl and has pro-apoptotic activity. *J Biol Chem* 2002;277:28870–28876. [PubMed: 12021275]
- Li T, Sham PC, Vallada H, Xie T, Tang X, Murray RM, Liu X, Collier DA. Preferential transmission of the high activity allele of COMT in schizophrenia. *Psychiatr Genet* 1996;6:131–133. [PubMed: 8902889]
- Lindsay EA, Vitelli F, Su H, Morishima M, Huynh T, Pramparo T, Jurecic V, Ogunrinu G, Sutherland HF, Scambler PJ, Bradley A, Baldini A. *Tbx1* haploinsufficiency in the DiGeorge syndrome region causes aortic arch defects in mice. *Nature* 2001;410:97–101. [PubMed: 11242049]
- Liu H, Abecasis GR, Heath SC, Knowles A, Demars S, Chen YJ, Roos JL, Rapoport JL, Gogos JA, Karayiorgou M. Genetic variation in the 22q11 locus and susceptibility to schizophrenia. *Proc Natl Acad Sci U S A* 2002a;99:16859–16864. [PubMed: 12477929]
- Liu H, Heath SC, Sobin C, Roos JL, Galke BL, Blundell ML, Lenane M, Robertson B, Wijsman EM, Rapoport JL, Gogos JA, Karayiorgou M. Genetic variation at the 22q11 *PRODH2/DGCR6* locus presents an unusual pattern and increases susceptibility to schizophrenia. *Proc Natl Acad Sci U S A* 2002b;99:3717–3722. [PubMed: 11891283]
- Maynard TM, Haskell GT, Peters AZ, Sikich L, Lieberman JA, LaMantia AS. A comprehensive analysis of 22q11 gene expression in the developing and adult brain. *Proc Natl Acad Sci U S A* 2003;100:14433–14438. [PubMed: 14614146]

- Meechan DW, Maynard TM, Wu Y, Gopalakrishna D, Lieberman JA, Lamantia AS. Gene dosage in the developing and adult brain in a mouse model of 22q11 deletion syndrome. *Mol Cell Neurosci* 2006;33:412–428. [PubMed: 17097888]
- Merscher S, Funke B, Epstein JA, Heyer J, Puech A, Lu MM, Xavier RJ, Demay MB, Russell RG, Factor S, Tokooya K, Jore BS, Lopez M, Pandita RK, Lia M, Carrion D, Xu H, Schorle H, Kobler JB, Scambler P, Wynshaw-Boris A, Skoultschi AI, Morrow BE, Kucherlapati R. TBX1 is responsible for cardiovascular defects in velo-cardio-facial/DiGeorge syndrome. *Cell* 2001;104:619–629. [PubMed: 11239417]
- Mukai J, Liu H, Burt RA, Swor DE, Lai WS, Karayiorgou M, Gogos JA. Evidence that the gene encoding ZDHHC8 contributes to the risk of schizophrenia. *Nat Genet* 2004;36:725–731. [PubMed: 15184899]
- Ohno Y, Kihara A, Sano T, Igarashi Y. Intracellular localization and tissue-specific distribution of human and yeast DHHC cysteine-rich domain-containing proteins. *Biochim Biophys Acta* 2006;1761:474–483. [PubMed: 16647879]
- Ousley O, Rockers K, Dell ML, Coleman K, Cubells JF. A review of neurocognitive and behavioral profiles associated with 22q11 deletion syndrome: implications for clinical evaluation and treatment. *Curr Psychiatry Rep* 2007;9:148–158. [PubMed: 17389127]
- Palmatier MA, Pakstis AJ, Speed W, Paschou P, Goldman D, Odunsi A, Okonofua F, Kajuna S, Karoma N, Kungulilo S, Grigorenko E, Zhukova OV, Bonne-Tamir B, Lu RB, Parnas J, Kidd JR, DeMille MM, Kidd KK. COMT haplotypes suggest P2 promoter region relevance for schizophrenia. *Mol Psychiatry* 2004;9:859–870. [PubMed: 15098000]
- Paterlini M, Zakharenko SS, Lai WS, Qin J, Zhang H, Mukai J, Westphal KG, Olivier B, Sulzer D, Pavlidis P, Siegelbaum SA, Karayiorgou M, Gogos JA. Transcriptional and behavioral interaction between 22q11.2 orthologs modulates schizophrenia-related phenotypes in mice. *Nat Neurosci* 2005;8:1586–1594. [PubMed: 16234811]
- Pomeroy SL, LaMantia AS, Purves D. Postnatal construction of neural circuitry in the mouse olfactory bulb. *J Neurosci* 1990;10:1952–1966. [PubMed: 2355260]
- Portnoi MF, Lebas F, Gruchy N, Ardalan A, Biran-Mucignat V, Malan V, Finkel L, Roger G, Ducrocq S, Gold F, Taillemite JL, Marlin S. 22q11.2 duplication syndrome: two new familial cases with some overlapping features with DiGeorge/velocardiofacial syndromes. *Am J Med Genet A* 2005;137:47–51. [PubMed: 16007629]
- Prabakaran S, Swatton JE, Ryan MM, Huffaker SJ, Huang JT, Griffin JL, Wayland M, Freeman T, Dudbridge F, Lilley KS, Karp NA, Hester S, Tkachev D, Mimmack ML, Yolken RH, Webster MJ, Torrey EF, Bahn S. Mitochondrial dysfunction in schizophrenia: evidence for compromised brain metabolism and oxidative stress. *Mol Psychiatry* 2004;9:684–697. 643. [PubMed: 15098003]
- Raux G, Bumsel E, Hecketsweiler B, van Amelsvoort T, Zinkstok J, Manouvrier-Hanu S, Fantini C, Breviere GM, Di Rosa G, Pustorino G, Vogels A, Swillen A, Legalic S, Bou J, Opolczynski G, Drouin-Garraud V, Lemarchand M, Philip N, Gerard-Desplanches A, Carlier M, Philippe A, Nolen MC, Heron D, Sarda P, Lacombe D, Coizet C, Alembik Y, Layet V, Afenjar A, Hannequin D, Demily C, Petit M, Thibaut F, Frebourg T, Campion D. Involvement of hyperprolinemia in cognitive and psychiatric features of the 22q11 deletion syndrome. *Hum Mol Genet* 2007;16:83–91. [PubMed: 17135275]
- Ryan AK, Goodship JA, Wilson DI, Philip N, Levy A, Seidel H, Schuffenhauer S, Oechsler H, Belohradsky B, Prieur M, Aurias A, Raymond FL, Clayton-Smith J, Hatchwell E, McKeown C, Beemer FA, Dallapiccola B, Novelli G, Hurst JA, Ignatius J, Green AJ, Winter RM, Brueton L, Brondum-Nielsen K, Scambler PJ, et al. Spectrum of clinical features associated with interstitial chromosome 22q11 deletions: a European collaborative study. *J Med Genet* 1997;34:798–804. [PubMed: 9350810]
- Schilling B, Murray J, Yoo CB, Row RH, Cusack MP, Capaldi RA, Gibson BW. Proteomic analysis of succinate dehydrogenase and ubiquinol-cytochrome c reductase (Complex II and III) isolated by immunoprecipitation from bovine and mouse heart mitochondria. *Biochim Biophys Acta* 2006;1762:213–222. [PubMed: 16120479]
- Shaner NC, Steinbach PA, Tsien RY. A guide to choosing fluorescent proteins. *Nat Methods* 2005;2:905–909. [PubMed: 16299475]
- Shifman S, Levit A, Chen ML, Chen CH, Bronstein M, Weizman A, Yakir B, Navon R, Darvasi A. A complete genetic association scan of the 22q11 deletion region and functional evidence reveal an

association between DGCR2 and schizophrenia. *Hum Genet* 2006;120:160–170. [PubMed: 16783572]

Sudo H, Tsuji AB, Sugyo A, Imai T, Saga T, Harada YN. A loss of function screen identifies nine new radiation susceptibility genes. *Biochem Biophys Res Commun* 2007;364:695–701. [PubMed: 17964541]

Wang G, Deschenes RJ. Plasma membrane localization of Ras requires class C Vps proteins and functional mitochondria in *Saccharomyces cerevisiae*. *Mol Cell Biol* 2006;26:3243–3255. [PubMed: 16581797]

Winterer G, Coppola R, Goldberg TE, Egan MF, Jones DW, Sanchez CE, Weinberger DR. Prefrontal broadband noise, working memory, and genetic risk for schizophrenia. *Am J Psychiatry* 2004;161:490–500. [PubMed: 14992975]

Wittig I, Karas M, Schagger H. High resolution clear native electrophoresis for in-gel functional assays and fluorescence studies of membrane protein complexes. *Mol Cell Proteomics* 2007;6:1215–1225. [PubMed: 17426019]

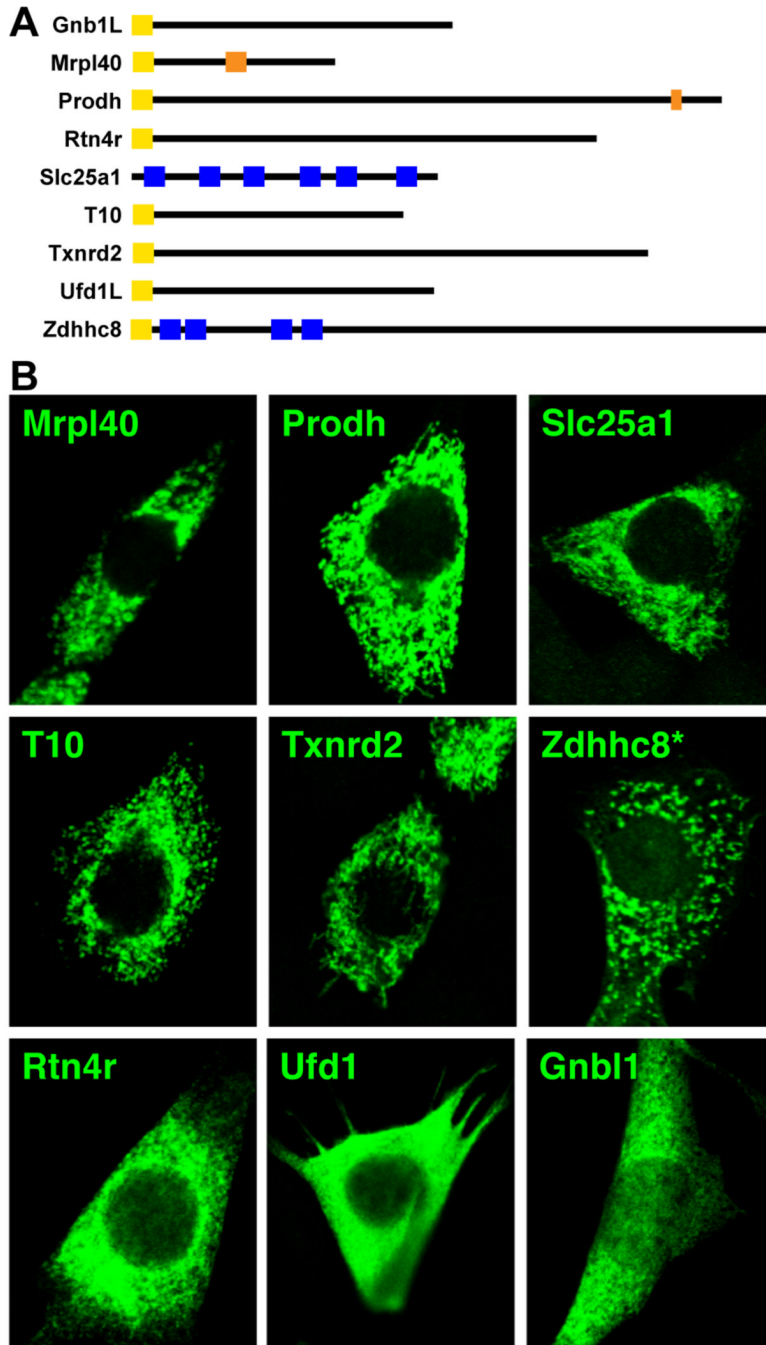


Figure 1. A subset of 22q11 genes is localized to mitochondria. Top: Schematic diagram shows the domain structure of putative mitochondrial 22q11 proteins predicted by informatic software. Yellow boxes are putative N-terminal mitochondrial localization signals, blue boxes are predicted transmembrane domains, and orange boxes are predicted nuclear localization signals. Bottom: Localization of expressed GFP fusions of all nine proteins. Six proteins (Mrpl40, Prodh, Slc25a1, T10, Txnrd2, Zdhhc8) show a punctate expression pattern consistent with mitochondrial localization, while three (Rtn4r, Ufd11, Gnb11) do not. Expression was examined in 3T3 cells after 36–40 hours, except Zdhhc8 (*), examined after 10 hours in primary mouse embryonic fibroblast cells (MEFs).

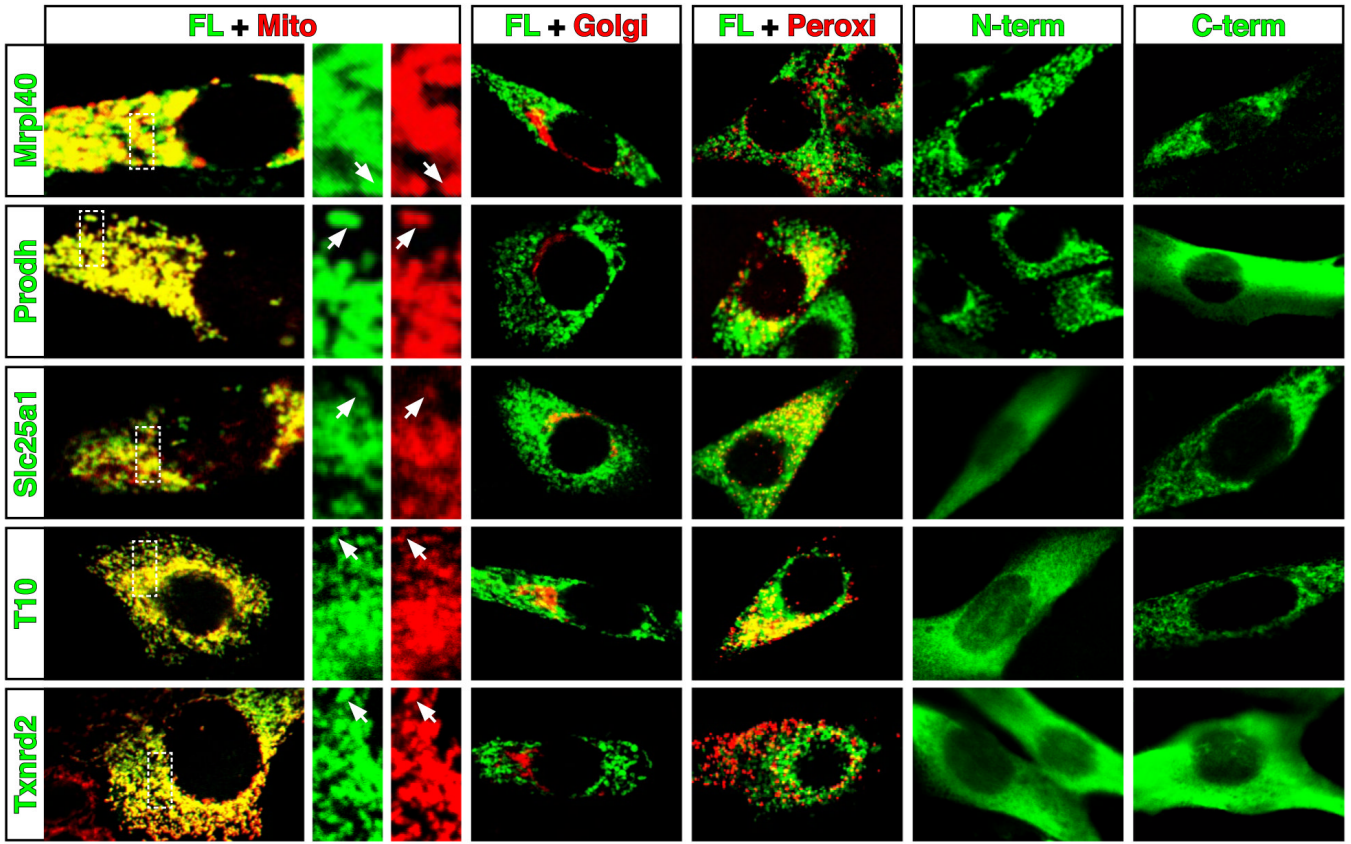


Figure 2. Multiple 22q11 proteins are specifically expressed in mitochondria. Presumptive mitochondrial 22q11 proteins have been overexpressed in parallel with several organelle specific reporter constructs and imaged as ~1 μ m optical sections. Left column: Co-localization of GFP fusions with full-length 22q11 proteins (green) with mitochondrially targeted mCherry fusion protein reporter constructs (red). Inset shows ~2.5x magnification of separated red and green channels. Columns 2 and 3: Co-expression of same full-length GFP fusions with golgi- and peroxisomally-targeted mCherry reporter constructs. Columns 4 and 5: Expression of GFP fusions with either N-terminal portion (putative mitochondrial targeting domain) or C-terminal (lacking targeting domain) portions of five mitochondrial proteins (see Supplementary Table 1). Zdhc8 proved cytotoxic when over-expressed, and thus was analyzed separately using alternative methods (see Figure 3).

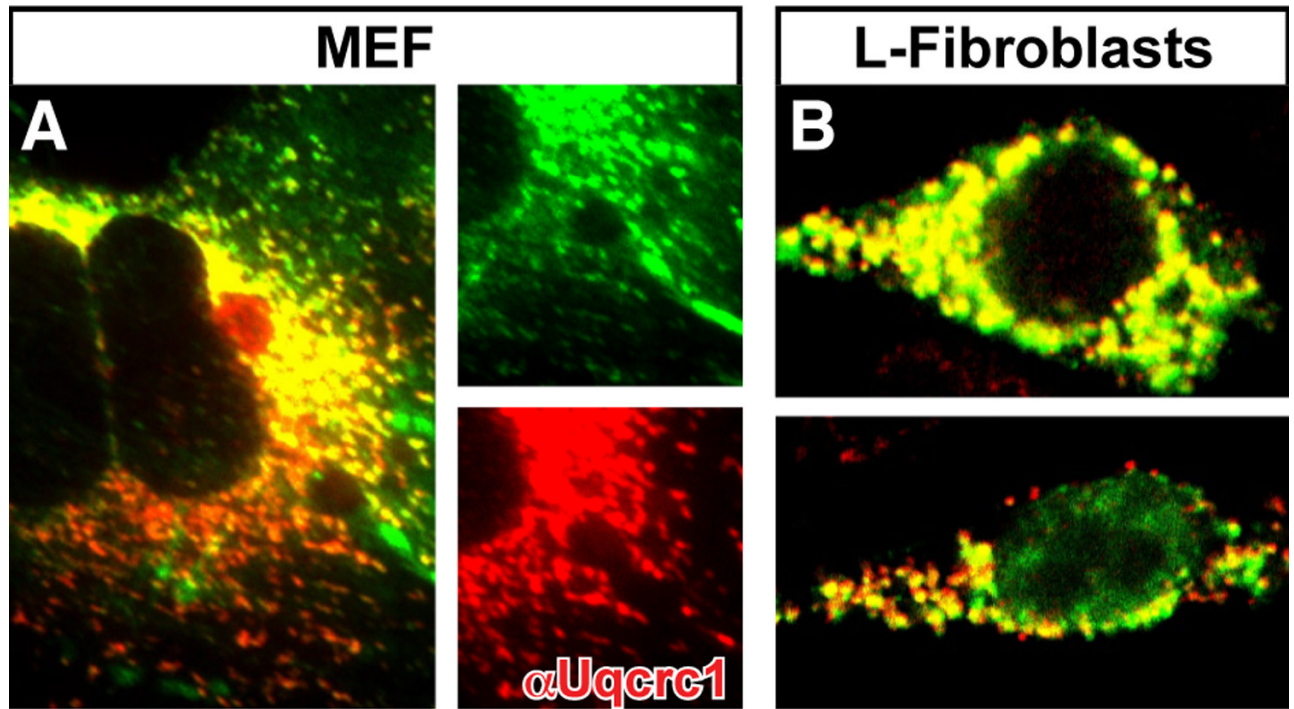


Figure 3. Zdhhc8 is found in mitochondria, and toxic when over-expressed. Immunolocalization of Zdhhc8 (green) in primary fibroblasts (MEFs, A) and a murine cell line (L-fibroblasts, B). Zdhhc8 expression coincides with mitochondria, as identified by Uqcrc1 immunolabeling (red).

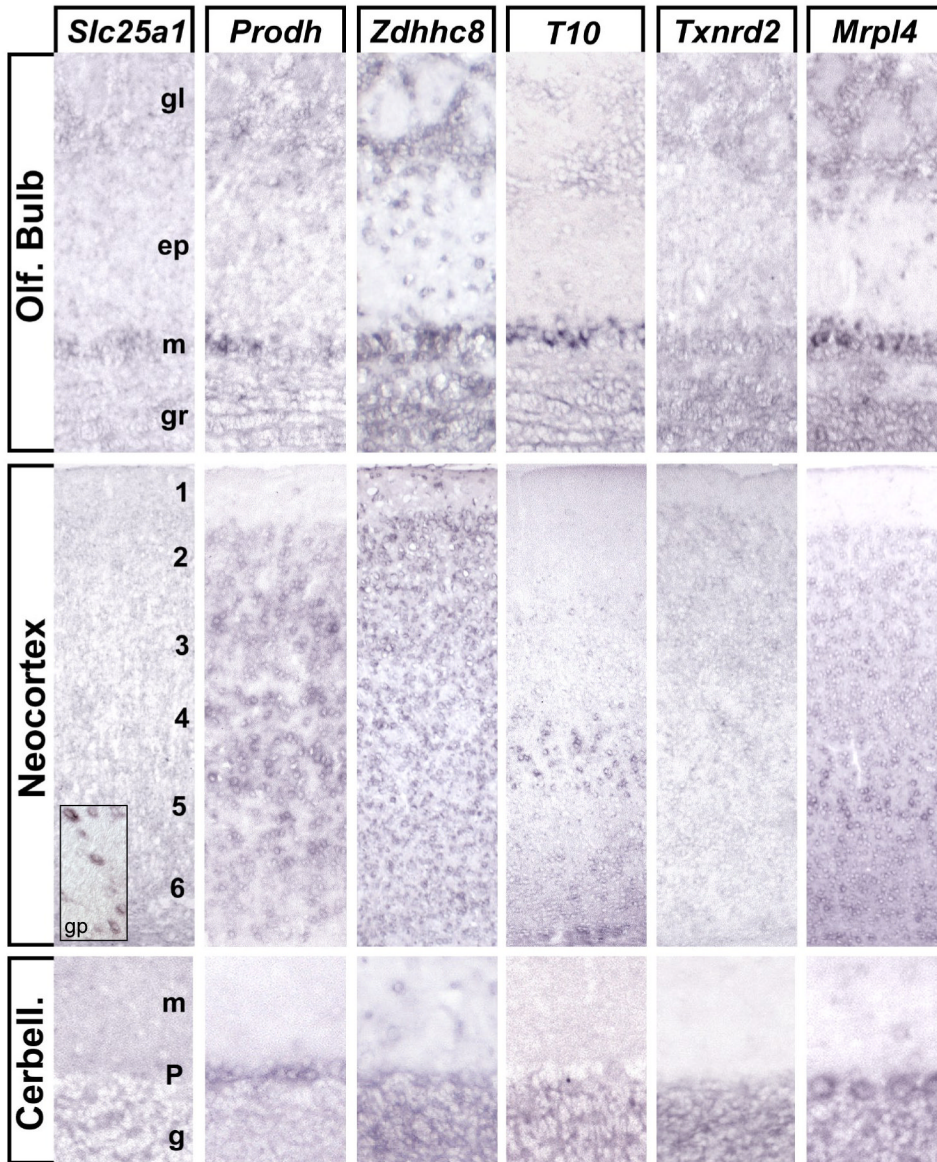


Figure 4.

Six mitochondrial 22q11 genes are expressed in distinct patterns and cell classes in the adult brain. Coronal sections through the olfactory bulbs, neocortex and cerebellum of adult (>P60) wild type mice have been hybridized for *Slc25a1*, *Prodh*, *Zdhhc8*, *T10*, *Txnrd2*, and *Mrpl40*. The characteristics layers of the olfactory bulbs, neocortex, and cerebellum are labeled in the panel at far left: for the olfactory bulb—glomerular layer, gl; external plexiform layer, ep; mitral cell layer, m; granule cell layer, gr; for the neocortex—numerals 1–6 represent the six neocortical layers, layer 1 is closest to the pia, layer 6 is closest to the subcortical white matter; for the cerebellum—molecular layer, m; Purkinje cell layer, P; granule cell layer, gr.

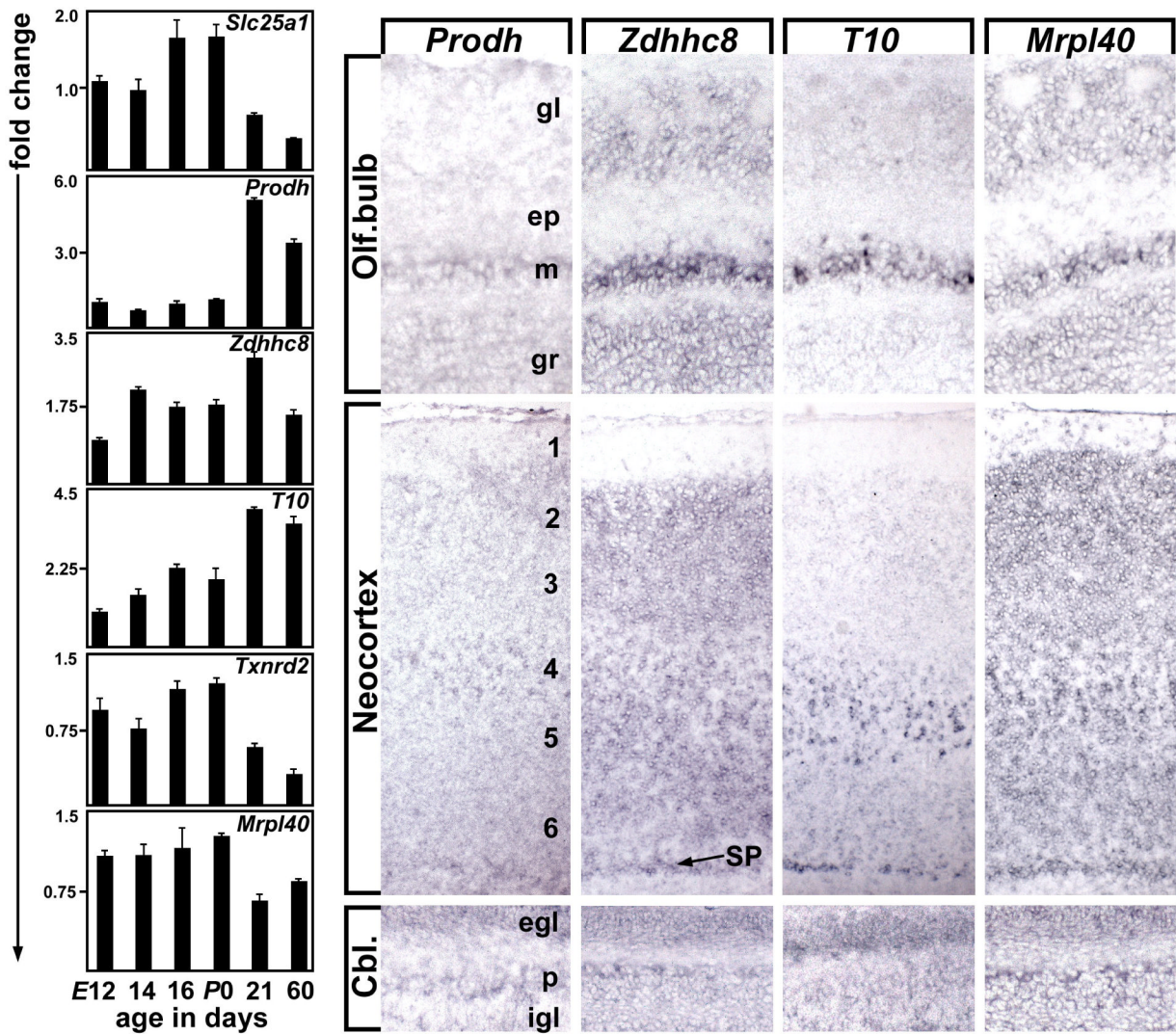


Figure 5.

The mitochondrial genes are maximally expressed during postnatal development, and acquire their adult distribution by shortly after birth. Left hand panel: Quantitative PCR analysis of relative levels of six mitochondrial 22q11 genes in embryonic (E12, 14, 16), postnatal (P0, P21) and adult (P60) whole brain. All reach an expression maximum at or shortly after birth, and expression levels of all decline once adulthood is reached. Right hand panel: Expression patterns of the four 22q11 genes that are significantly expressed in the adult brain (see Figure 4) at P10. In each case, there is robust expression, and the basic cellular distribution seen in the adult is in place by this mid post-natal age. In addition, expression is seen in two transient cellular compartments that characterize either the developing neocortex—the subplate, (SP, arrow) or the cerebellum—the external granule cell layer (egl).

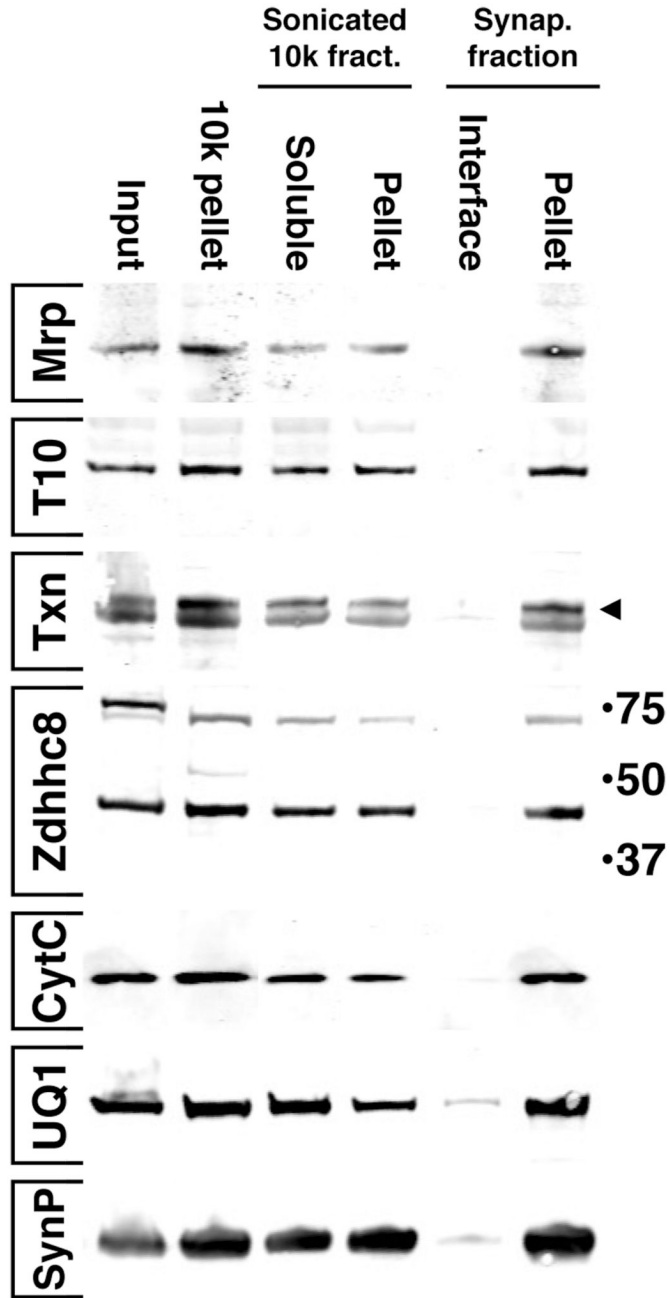


Figure 6. 22q11 mitochondrial proteins are enriched in brain mitochondria, and synapses. Immunoblot analysis of 22q11 protein expression in fractionated lysates of adult mouse brain. Input lysates (Input) were fractionated produce a crude mitochondrial fraction (10k pellet); this was then examined for solubility of individual proteins by sonication, followed by an additional centrifugation to determine whether the protein was released into the soluble fraction (Soluble) or remained insoluble (Pellet). Additionally, the crude lysate fraction was purified using a sucrose step gradient to enrich for synaptosomes (Synap. fraction); the interface contains non-synaptosomal protein, while the synaptosomes are collected in the pellet. Four 22q11 proteins were assayed; Zdhhc8, Mrpl40 (Mrp), T10, and Txnrd2. Txnrd2 immunolabeling identified

two bands, the lower band is artifactual. Two mitochondrial markers, Cytochrome C (CytC) and Uqcrc1 (UQ1), and a synaptic marker, Synaptophysin (SynP) are assayed to validate the quality of the samples.

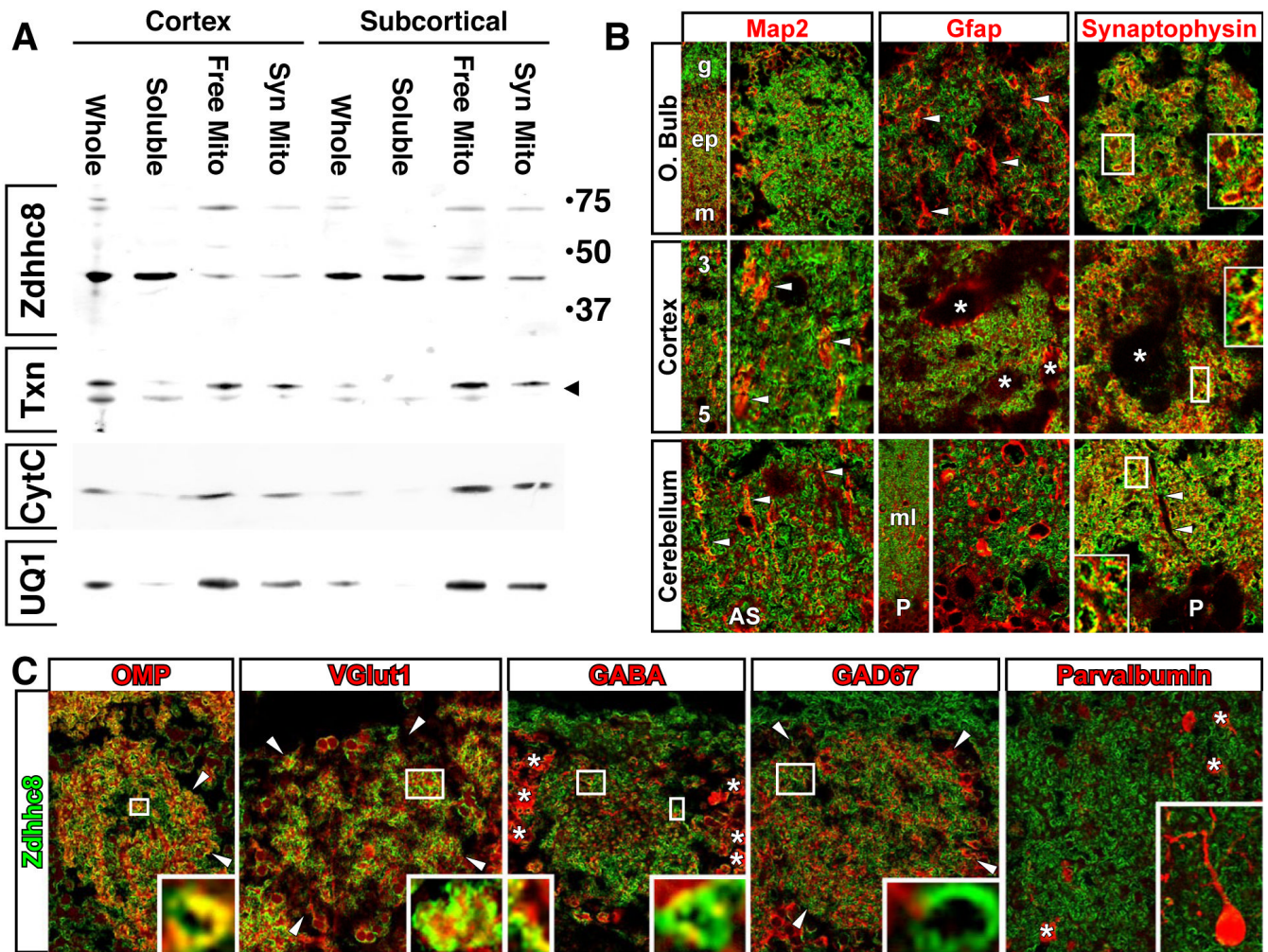


Figure 7.

Enrichment of 22q11 proteins in cortical mitochondria. **(A)** To further clarify the localization of 22q11 proteins in brain mitochondria, two brain regions (cortical and subcortical forebrain regions) were lysed (whole), and centrifuged to separate the soluble (non mitochondrial) fraction (soluble) from the synaptosome and mitochondria containing fraction. This latter fraction was further fractionated to yield both free mitochondria (Free mito), and mitochondria associated with synaptosomes (Syn mito). **(B)** Zdhhc8 puncta correspond to presynaptic processes. The olfactory bulb, cortex, and cerebellum have been labeled for Zdhhc8 (green) and Map2, GFAP, and Synaptophysin (red) to assess coincident expression in dendrites, presynaptic endings, and glial cells and processes respectively. Low and high magnification images show that there is no significant overlap of neuronal cell bodies or processes that express either GFAP or the microtubule associated protein 2 (Map2). Glial processes labeled with GFAP or dendrites labeled for Map2 (arrowheads) in the mitral cell layer (m), external plexiform layer (ep), or glomerular layer (g) of the olfactory bulb are distinct from the Zdhhc8 puncta. This is also the case in the middle layers (3, 5) of the cerebral cortex, and the molecular layer (ml) of the cerebellum where astrocyte cell bodies (AS) are also seen. Synaptophysin colocalizes closely with Zdhhc8. Like Zdhhc8, synaptophysin is mostly excluded from cell bodies and dendrites (unlabelled regions in all three panels at far right; neocortical cell bodies indicated with asterisk, cerebellar Purkinje cell indicated with P, apical Purkinje cell dendrite indicated by arrowheads). The characteristic “ring” pattern is seen in the staining for both Zdhhc8 and

synaptophysin (insets, far right). (C) Zdhhc8 is seen in both excitatory and inhibitory presynaptic processes. Glomeruli in the olfactory bulb (g), which include excitatory and inhibitory presynaptic endings, have been double-labeled for Zdhhc8 and OMP (which labels glutamatergic primary afferents from the olfactory receptor neurons), Vglut1 (the vesicular glutamate transporter 1, broadly associated with CNS glutamatergic presynaptic endings), GABA, and the GABA synthetic enzyme GAD67. Parvalbumin, which characterizes subsets of GABAergic interneurons in the external plexiform layer of the bulb, has also been localized in parallel with Zdhhc8 (far right panel). Arrowheads indicate the limits of the glomeruli for the OMP, Vglut1, GAD67 panels. Asterisks indicate the GABA-labeled periglomerular cells that define the glomerular boundaries in the GABA panel. Varying degrees of co-localization of Zdhhc8 is seen for OMP, Vglut1, and GABA, and the patterns are once again in the “ring” configuration (insets; OMP, Vglut1, GABA, GAD). There is no apparent co-localization for Parvalbumin and Zdhhc8 in the external plexiform layer. The inset shows a Parvalbumin labeled periglomerular interneuron and local parvalbumin puncta that are distinct from the Zdhhc8 puncta.

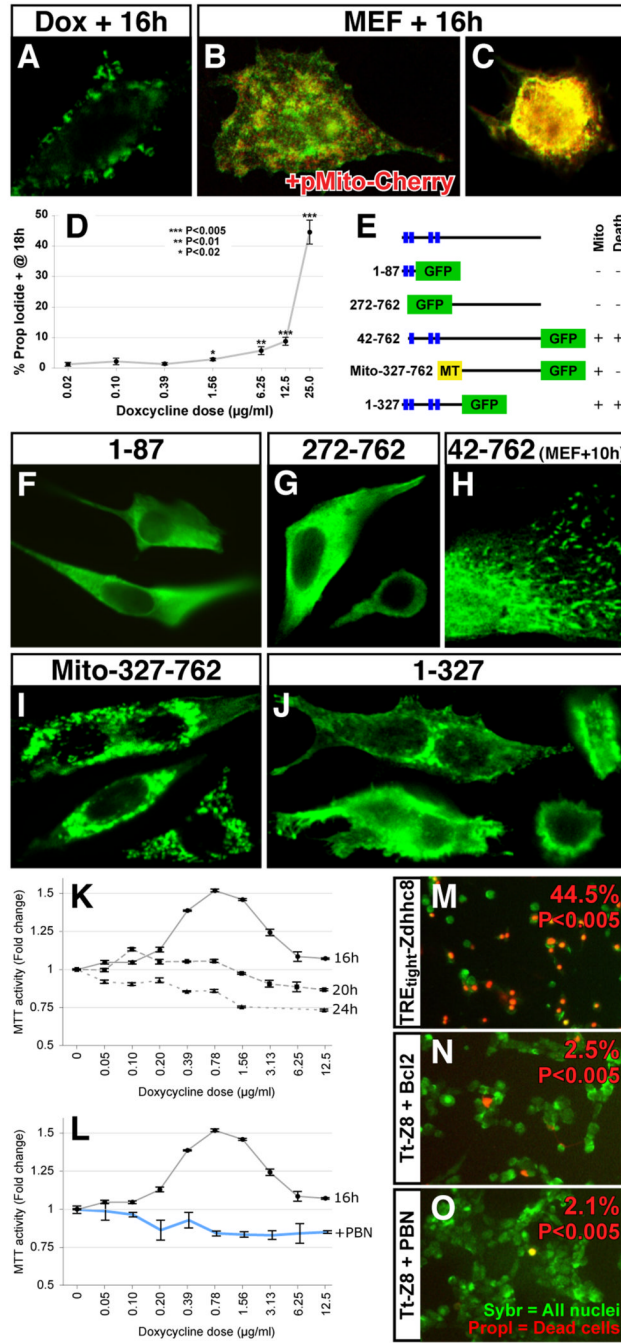


Figure 8. Zdhhc8 overexpression is toxic to cells. (A) 16 hours of overexpression at a moderate dose (using a tetracycline responsive promoter element) leads to Z8-EGFP accumulation in dysmorphic mitochondria in 3T3 cells. (B, C) Expression of Z8-EGFP using a CMV promoter in primary fibroblasts for 16 hours yields dysmorphic cells, with no distinct mitochondrial profiles labeled either with pZdhhc8-eGFP or pCherry-Mito (D) Zdhhc8 induced cell death is dose dependent in a doxycycline-inducible-Zdhhc8 expressing 3T3 cell line. Proportion of propidium iodide labeled nuclei after 18h induction by varying doses of doxycycline; significant levels of cell death are observed at the four highest doses, increasing to 44.5% at the highest dose (see also M). (E) Schematic of constructs used to assess Zdhhc8 function.

(F–J) Expression of GFP fusions of fragments of Zdhhc8 in 3T3 cells at 12–16 hours (except H): **(F)** putative targeting sequence, **(G)** C-terminal fragment, **(H)** Zdhhc8 lacking putative targeting sequence (shown in primary fibroblasts at 10 hours to show mitochondrial localization), **(I)** C-terminal fragment with additional mitochondrial targeting signal added, and **(J)** N-terminal fragment. C-terminus, not including predicted signal region, is targeted to mitochondria, and is toxic; N-terminal fragments are not localized to mitochondria without addition of ectopic signal sequence, and are not toxic. **(K)** MTT metabolism is altered by expression of Zdhhc8 in doxycycline inducible line. MTT metabolism (relative to untreated cells) was measured after 16, 20, and 24 hours following addition of varying doses of doxycycline; a transient increase was seen at intermediate dosages at 16 hours, while a general decrease in metabolism was observed at 20 and 24 hours. **(L)** The transient increase in MTT metabolism at 16 hours was blocked by the addition of 50 μ M N-t-butyl-phenylnitron (PBN). **(M)** Normal cell death observed at 18 hours following high-dose doxycycline treatment (see also D) was significantly diminished in cells co-expressing the anti-apoptotic factor Bcl2 **(N)**, as well as in cells treated with 50 μ M PBN **(O)**.

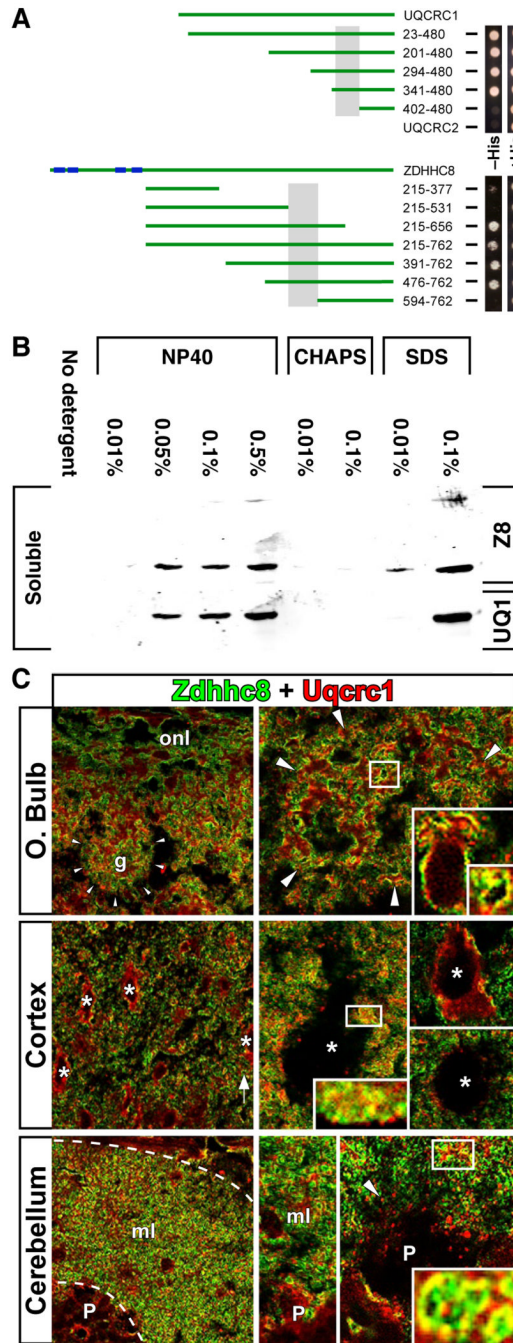


Figure 9.

A 22q11 mitochondrial protein, Zdhhc8, can physically interact with an mitochondrial core complex protein, Uqcrc1. (A) Schematic of two-hybrid analysis of Zdhhc8 tail domain (AA 215-762) with deletion fragments of Uqcrc1 (top), or Uqcrc1 (AA 23-480) with deletion fragments of Zdhhc8. Right columns show growth of reporter yeast transformed with both plasmids on selective (-His) or non-selective (+His) growth media (-Leu/-Trp). (B) Detergent solubility of brain mitochondrial fractions. Crude brain mitochondrial fractions (16k pellet) were treated with different concentrations of NP40, CHAPS, or SDS for 20 minutes, then re-centrifuged for 10 minutes at 16k xg. Soluble fractions were then assayed for presence of Zdhhc8 or UQCRC1 (UQ1). (C) Zdhhc8 is expressed primarily in presynaptic terminals.

Zdhhc8 (green) has been colocalized Uqcrc1 in the CNS (red). Punctate expression of Zdhhc8 is seen in confocal micographs of neuropil rich glomeruli (g, indicated by arrowheads) in the olfactory bulb (O.bulb; the olfactory nerve fiber layer, onl, indicates the outer surface of the bulb). The Zdhhc8 puncta are also seen in the neocortex (Cortex); however Zdhhc8 appears to be excluded from cortical cell bodies (asterisks; the arrow in the lower right hand corner indicates the direction to the pial surface). In the cerebellum, Zdhhc8 and Uqcrc1 coincide in the molecular layer (ml, a cerebellar folium is indicated with dotted line); however Zdhhc8 is not seen in the Purkinje cell layer (P). Zdhccc8 is often seen in either rings or clusters (insets) where it coincides extensively, but not completely, with Uqcrc1.

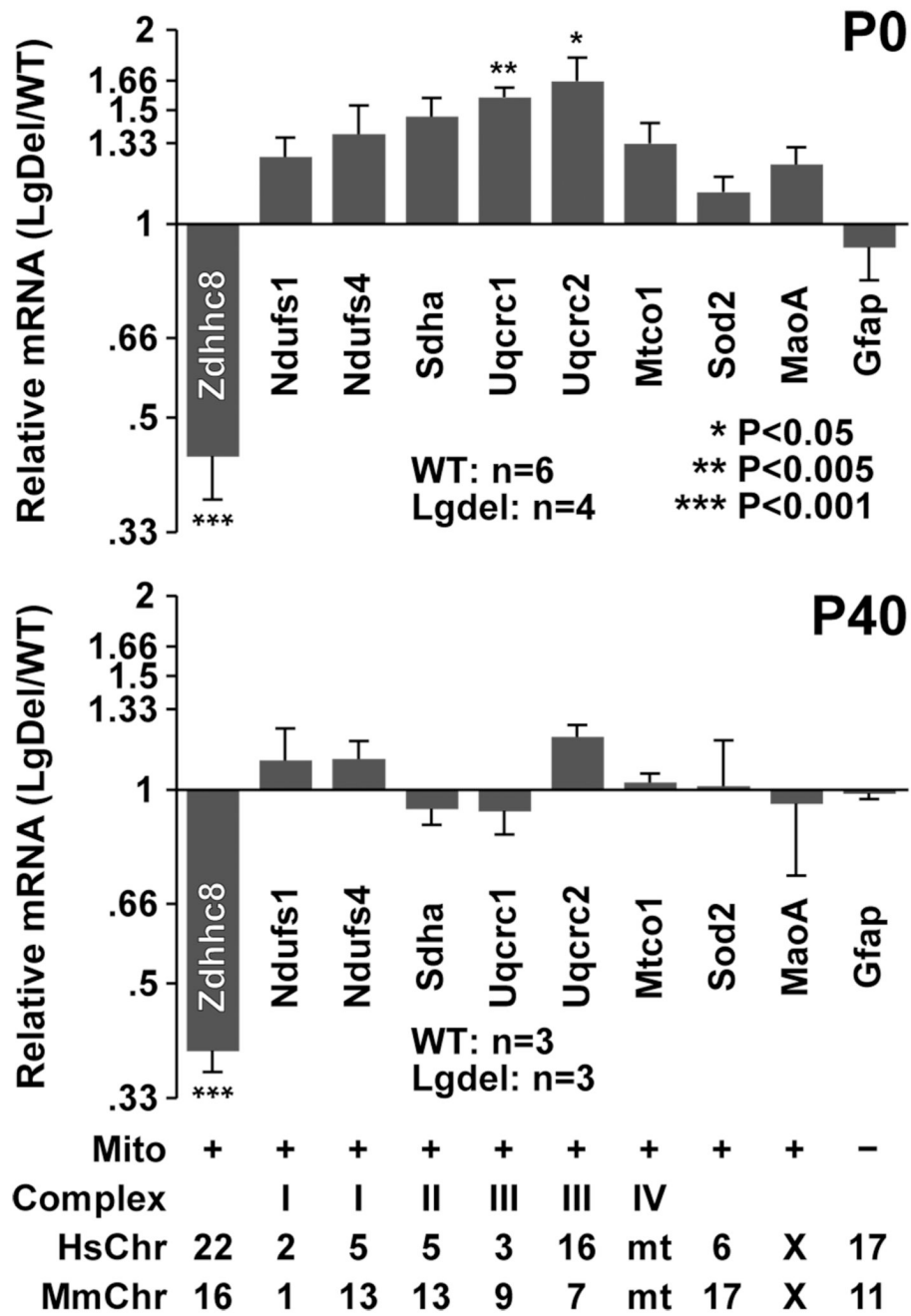


Figure 10.